Molecular Pharmacology Fast Forward. Published on May 15, 2007 as doi:10.1124/mol.106.032458

GLITAZONES INDUCE ASTROGLIOMA CELL DEATH BY RELEASING REACTIVE OXYGEN SPECIES FROM MITOCHONDRIA: MODULATION OF CYTOTOXICITY BY NITRIC OXIDE

José M. Pérez-Ortiz, Pedro Tranque, Miguel Burgos, Cecilia F. Vaquero and Juan Llopis

Physiology Unit, Facultad de Medicina, and Centro Regional de Investigaciones Biomédicas (CRIB), Universidad de Castilla-La Mancha, 02006 Albacete, Spain

Molecular Pharmacology Fast Forward. Published on May 15, 2007 as DOI: 10.1124/mol.106.032458
This article has not been copyedited and formatted. The final version may differ from this version.

Running title: Origin of glitazone-induced ROS in astroglioma cells.

Corresponding author: Juan Llopis, Facultad de Medicina, Universidad de Castilla-La Mancha, Avenida de Almansa 14, 02006 Albacete, Spain. Tel.: +34-967-599315; Fax: +34-967-599327; E-mail: Juan.llopis@uclm.es

Number of text pages: 29

Number of tables: 0

Number of figures: 7

Number of supplemental figures: 6, plus supplemental methods

Number of supplemental videos: 1

Number of references: 40

Number of words in the Abstract: 250

Number of words in the Introduction: 610

Number of words in the Discussion: 1327

Abbreviations: FCCP, Carbonylcyanide p-trifluoromethoxyphenyl-hydrazone; DAF-2 DA, 4,5-diaminofluorescein diacetate; DCF, 2',7'-dichlorofluorescein; H_2DCF, dichlorodihydrofluorescein; H_2DCF-DA, dichlorodihydrofluorescein diacetate; DMNQ, dimethoxynaphtoquinone; HE, hydroethidine; H_2O_2, hydrogen peroxide; L-NAME, N(G)-nitro-L-arginine methyl ester; LPS, lipopolysaccharide; NO, nitric oxide; NOS, nitric oxide synthase; $ONOO^-$, peroxynitrite; PPARγ, peroxisome proliferative activator receptor-γ; PI, propidium iodide; ROS, reactive oxygen species; S.D., standard deviation; $O_2^{\cdot -}$, superoxide anion; GSNO, S-Nitrosoglutathione; TMRE, tetramethylrhodamine ethyl ester perchlorate; TNFα, tumor necrosis factor-alpha; ΔΨm, mitochondrial membrane potential.

Molecular Pharmacology Fast Forward. Published on May 15, 2007 as DOI: 10.1124/mol.106.032458
This article has not been copyedited and formatted. The final version may differ from this version.

ABSTRACT

The glitazones (or thiazolidinediones) are synthetic compounds used in type-2 diabetes, but they also have broad anti-proliferative and anti-inflammatory properties still not well understood. Previously we described the apoptotic effects of glitazones on astroglioma cells (J. Biol. Chem., 279, 8976-8985). At certain concentrations, we found a selective lethality on glioma cells versus astrocytes, which was dependent on a rapid production of reactive oxygen species (ROS) and seemed unrelated to the receptor PPARγ. The present study was aimed at characterizing the oxygen derivatives induced by ciglitazone, rosiglitazone and pioglitazone in C6 glioma cells and to investigate their intracellular source. We examined the interaction of ROS with nitric oxide (NO) and its consequences for glioma cell survival. Fluorescence microscopy and flow cytometry showed that glitazones induced superoxide anion, peroxynitrite and hydrogen peroxide, ciglitazone being the most active. ROS production was completely prevented by uncoupling of the electron transport chain and by removal of glucose as energy substrate, whereas it was unaffected by inhibition of NADPH-oxidase and xanthine-oxidase. Moreover, glitazones inhibited state 3 respiration in permeabilized cells, and experiments with mitochondrial inhibitor suggested that Complex-I was the likely target of glitazones. Therefore, these results point to the mitochondrial electron transport chain as the source of glitazone-induced ROS in C6 cells. Glitazones also depolarized mitochondria and reduced mitochondrial pH. NO synthase inhibitors revealed that superoxide anion combines with NO to yield peroxynitrite, and that the latter contributes to the cytotoxicity of glitazones in astroglioma cells. Future anti-tumoral strategies may take advantage of these findings.

Molecular Pharmacology Fast Forward. Published on May 15, 2007 as DOI: 10.1124/mol.106.032458
This article has not been copyedited and formatted. The final version may differ from this version.

The glitazones, also called thiazolidinediones, constitute a group of synthetic compounds with insulin-sensitizing effects. Two members of this family, rosiglitazone and pioglitazone, are approved for the treatment of hyperglycemia in type 2 diabetes mellitus. In most countries they are used as monotherapy or in combination with sulfonylureas or metformin, and in the United States they are approved to use in combination with insulin (Yki-Jarvinen, 2004). Although the application of glitazones in the clinic is presently limited to diabetes, their potential therapeutic value expands beyond the regulation of the carbohydrate and lipid metabolisms since a growing number of reports have described that glitazones also affect vascular functions, inflammatory processes, cell proliferation and apoptosis (Feinstein *et al.*, 2005).

Many metabolic and anti-inflammatory properties of glitazones are linked to the activation of the peroxisome proliferator activated receptor-γ (PPARγ), a transcription factor of the nuclear receptor family that not only stimulates, but also represses a number of genes (Delerive *et al.*, 2001). However, alternative PPARγ-independent mechanisms are now emerging to account for a set of glitazone responses (Feinstein *et al.*, 2005), including antiproliferative and apoptotic actions on several tumor cells in vitro, in animal models and in humans (Grommes *et al.*, 2004).

Recently we demonstrated that the glitazones ciglitazone and rosiglitazone reduce the viability of astroglial cells (Perez-Ortiz *et al.*, 2004). This cytotoxic effect was cell-type dependent, as both glitazones affected preferentially astroglioma cell survival when compared to primary rat astrocytes. The mechanism involved in this anti-tumoral effect was clearly not mediated by PPARγ, but seemed related to an acute generation of reactive oxygen species (ROS) from an unknown cellular source.

Mitochondria are major producers of ROS in response to agents that alter their functions. Interestingly, our preliminary studies found that glitazones can cause

Molecular Pharmacology Fast Forward. Published on May 15, 2007 as DOI: 10.1124/mol.106.032458
This article has not been copyedited and formatted. The final version may differ from this version.

mitochondrial membrane depolarization both in glioma cells and astrocytes, pointing to mitochondria as a target of glitazones. In fact, glitazones have been reported to affect mitochondria in hepatoma cells (Masubuchi *et al.*, 2006), Jurkat and Raji cells (Kanunfre *et al.*, 2004) and human multiple myeloma, among others (Ray *et al.*, 2004). Moreover, glitazones have been shown to generate ROS as a result of the modulation of mitochondrial functions in several cell types (Narayanan *et al.*, 2003). Alternatively, glitazones could stimulate ROS production from extramitochondrial sources, i.e. by xanthine-oxidase and NADPH-oxidase, enzymes known to be expressed in astrocytes.

Although we found that ROS are implicated in the lethal effect of glitazones on glioma cells, a matter that still needed clarification is the type of oxygen derivatives released. Superoxide anion ($O_2^{\cdot -}$) is a short-lived ROS generated as a by-product of oxidative phosphorylation in mitochondria, or alternatively as a result of the activity of the cytosolic oxidases mentioned before. It can be metabolized to hydrogen peroxide (H_2O_2) by dismutation or converted into peroxynitrite ($ONOO^-$) by combination with NO. In relation to this, the expression of different isoforms of the NO synthase (NOS) in C6 glioma cells has been reported. Both $O_2^{\cdot -}$ derivatives, H_2O_2 and $ONOO^-$, have deleterious effects on cells and could mediate the cytotoxicity of glitazones. NOS activity might modulate glioma cell death caused by glitazones, since H_2O_2 and $ONOO^-$ are expected to induce different levels of toxicity (Radi *et al.*, 2002).

In consequence, the present report was aimed at understanding the actions of glitazones on C6 glioma cells. In particular, we characterized the type of ROS generated in response to glitazones and their subcellular origin. In addition, we addressed the implications of modulating NO levels for the cell lethality induced by glitazones. Our findings indicate a rather selective action of glitazones on mitochondria vs. other ROS sources, and contribution of both $O_2^{\cdot -}$ and $ONOO^-$ to glitazone cytotoxicity in C6 glioma cells.

Molecular Pharmacology Fast Forward. Published on May 15, 2007 as DOI: 10.1124/mol.106.032458
This article has not been copyedited and formatted. The final version may differ from this version.

MATERIALS AND METHODS

Reagents

Ciglitazone {5-[[4-[(1-methylcyclohexyl)methoxy]phenyl]methyl]-1,3-thiazolidine-2,4-dione} and carbonyl cyanide 4-(trifluoromethoxy)phenylhydrazone (FCCP) were purchased from Tocris. Rosiglitazone {5-[[4-[2-(methyl-pyridin-2-yl-amino)ethoxy]phenyl]methyl]thiazolidine-2,4-dione}, pioglitazone {5-[[4-[2-(5-ethylpyridin-2-yl)ethoxy]phenyl]methyl]thiazolidine-2,4-dione}, 1400W and S-Nitrosoglutathione (GSNO) were obtained from Alexis. All the fluorescent probes used (dichlorodihydrofluorescein diacetate, H_2DCF-DA; hydroethidine, HE; tetramethylrhodamine ethyl ester, TMRE) were purchased from Molecular Probes, except 4,5-diaminofluorescein diacetate (DAF-2 DA) which was a generous gift of Dr. Kazuya Kikuchi (Osaka University, Japan). Apocynin was acquired from Calbiochem. Trypsin-EDTA, DMEM-F12, fetal bovine serum and antibiotics were obtained from Cambrex. Mouse anti-nitrotyrosine antibody was purchased from Hycult Biotechnology (The Netherlands) and sheep anti-mouse IgG-horseradish peroxidase (HRP) was from Amersham Bioscience (UK). All other chemicals and inhibitors were purchased from Sigma.

Rat C6 glioma cells

The rat astroglioma cell line C6 was cultured in Dulbecco's modified Eagle's medium-F12, supplemented with 10% fetal bovine serum and antibiotics. Experimental treatments were applied to 60-70% confluent cultures.

Measurement of mitochondrial membrane potential

Molecular Pharmacology Fast Forward. Published on May 15, 2007 as DOI: 10.1124/mol.106.032458
This article has not been copyedited and formatted. The final version may differ from this version.

C6 cells were grown in 22 mm round coverslips and 24-36 hours after seeding cells were washed twice with Hanks' balanced salt solution (HBSS) containing 5 mM glucose and 10 mM HEPES, pH 7.4. Cells were loaded with 0.1 μM TMRE for 20 min at room temperature and protected from direct light. After that, coverslips were transferred to a microscopy chamber (Attofluor, Molecular Probes, The Netherlands) and maintained in the presence of 0.1 μM TMRE. Cell fluorescence was imaged with an epifluorescence inverted microscope (DMIRE-2, Leica, Germany) equipped with an oil immersion 40x objective (NA 1.25). Excitation light at 545 nm was obtained using a monochromator (Hamamatsu Photonics, Japan) and emitted light was collected by a CCD camera (Orca-ER, Hamamatsu Photonics). The interference filter used for emission was 635 ± 27 nm and the dicroic mirror was 570DRL (Omega Optical, USA). Regions of interest (nucleus and cytoplasm) were selected manually, and pixel intensities were spatially averaged after background subtraction. A binning of two was used to improve signal/noise and minimize photobleaching of TMRE and photodamage to the cells. All images and data were acquired and analyzed using the Aquacosmos software (Hamamatsu Photonics).

Detection of intracellular ROS by microscopy and flow cytometry

Cells were incubated with the cell permeant dye H_2DCF-DA, which intracellularly de-esterifies to dichlorodihydrofluorescein (H_2DCF). Reactive oxygen species (ROS) oxidize H_2DCF to the brightly green fluorescent compound 2',7'-dichlorofluorescein (DCF), which was monitored by microscopy and flow cytometry following methods described previously (Perez-Ortiz *et al.*, 2004). For microscopy, C6 cells were grown in 22 mm round coverslips and 24-36 hours after seeding, cells were incubated during 30 min with 20 μM of the corresponding glitazone at 37ºC in serum-free DMEM-F12. Within the last 15 min of glitazone treatment, cells were loaded with 1 μM H_2DCF-DA. Afterwards, coverslips were

Molecular Pharmacology Fast Forward. Published on May 15, 2007 as DOI: 10.1124/mol.106.032458
This article has not been copyedited and formatted. The final version may differ from this version.

transferred to a microscopy chamber and maintained in HBSS containing 2 mM calcium and 10 mM HEPES, pH 7.4. Cell fluorescence was imaged with the same setup and software described above, using 480 nm excitation (monochromator), 505DRL dicroic mirror and 535 ± 26 nm emission filter. A binning of four was used to minimize photobleaching of DCF.

For flow cytometry, cells treated with glitazones or vehicle (Me_2SO) were incubated with 2.5 μM H_2DCF-DA for 15 min at 37°C, detached from the plate with trypsin/EDTA, washed with phosphate buffered saline, resuspended in 1 ml DMEM-F12 with 2% FBS and placed on ice protected from light. The intensity of the fluorescent DCF in the cell suspension was measured immediately by a BD-LSR flow cytometer (Becton Dickinson) equipped with an Argon ion laser (488 nm excitation); the emission filter was set at 530 nm. Triplicate samples were run in each experiment, and at least 10000 cells per sample were analyzed. Mean fluorescence was calculated with the program CellQuest (Becton Dickinson). Dead cells and debris were excluded from the analysis by electronic gating of forward- and side-scattering measurements.

Hydroethidine staining assay for superoxide formation

Superoxide anion was measured with the fluorescent dye hydroethidine (HE). This probe is oxidized to ethidium which is trapped by intercalating with DNA resulting in a fluorescence signal that can be quantified by flow cytometry. C6 cells were grown in complete DMEM-F12 and washed with PBS before treatment. Subsequently, cells were incubated during 15 minutes with 5 μM HE in serum-free DMEM-F12 and then treated with each glitazone for 15 min. Afterwards, cells were detached from the culture plate with trypsin/EDTA, resuspended in 1 ml DMEM-F12 with 2% FBS, protected from light and placed on ice. The intensity of the fluorescent ethidium was measured immediately by a BD-LSR flow cytometer (Becton Dickinson) equipped with an Argon ion laser (488 nm excitation); the emission filter was set

Molecular Pharmacology Fast Forward. Published on May 15, 2007 as DOI: 10.1124/mol.106.032458
This article has not been copyedited and formatted. The final version may differ from this version.

at 575 nm. For imaging HE, cells were loaded with 5 μM HE for 10 min at 37ºC in an incubator. After that, coverslips were transferred to a microscopy chamber and maintained in HBSS. Cell fluorescence was imaged with the setup described before. Excitation light was at 397 nm and emission was collected with a 595 nm emission filter. Regions of interest were selected manually, and pixel intensities were spatially averaged after background subtraction. A binning of two was used to improve signal/noise and minimize photobleaching of HE. All images and data were acquired and analyzed using the Aquacosmos software (Hamamatsu Photonics).

Mitochondrial respiration

Oxygen consumption of digitonin-permeabilized cells was monitored polarographically with a Clark-type oxygen electrode (Oxygraph, Hansatech Instruments) connected to a suitable recorder in a 1-ml thermostatted water-jacketed closed chamber with magnetic stirring. The reactions were carried out at 30°C in 1 ml of the standard medium (225 mM sucrose, 10 mM KCl, 5 mM $MgCl_2$, 10 mM KH_2PO_4 / K_2HPO_4, 0.1% BSA, 1 mM EGTA, 10 mM Tris-HCl, pH 7.4) containing 10^7 cells. 5 mM pyruvate/2.5 mM malate and 250 μM ADP were added to achieve state 3 of respiration.

NO analysis with DAF-2

NO production was assayed using the fluorescent probe 4,5-diaminofluorescein (DAF-2). C6 cells were grown in complete DMEM-F12. After washing with PBS, cells were incubated with 5 μM DAF-2 DA in DMEM-F12 serum-free for 15 min followed by addition of glitazone for another 15 min. Cell fluorescence was analyzed by a BD-LSR flow cytometer (Becton Dickinson). Excitation was at 488 nm (Ar ion laser) and the emission filter was centered at 530 nm.

Molecular Pharmacology Fast Forward. Published on May 15, 2007 as DOI: 10.1124/mol.106.032458
This article has not been copyedited and formatted. The final version may differ from this version.

Cell viability by propidium iodide exclusion

This assay is based on the exclusive nuclear labelling of nonviable cells with the DNA intercalating fluorescent dye propidium iodide. C6 glioma cells were harvested with trypsin and stained with 10 μg/ml propidium iodide prior analysis by flow cytometry. Fluorescence was excited at 488 nm and measured through a 575/26 band-pass filter.

Western blotting

Cell lysates were loaded onto sodium dodecyl sulphate (SDS)–polyacrylamide gels, electrophoresed and subsequently transferred to polyvinylidene fluoride membranes (Pall, Ann Harbor, MI, USA), incubated with anti-β-actin (1:2000) or anti-nitrotyrosine (1:50) antibodies and probed with peroxidase-conjugated secondary antibody following manufacturer's instructions. An enhanced chemiluminescence system was used for visualization.

Statistical analysis

Results are expressed as percentage of controls treated with the appropriate vehicle (Me_2SO). Values represent mean ± standard deviation (S.D.) of 3–6 replicate wells. Data were analyzed by one-way analysis of variance followed by a Least Significant Differences test. Statistical significance of differences vs. respective controls is shown ($^{\#}$, $p<0.05$; *, $p<0.01$; **, $p<0.001$; ***, $p<0.0001$).

Molecular Pharmacology Fast Forward. Published on May 15, 2007 as DOI: 10.1124/mol.106.032458
This article has not been copyedited and formatted. The final version may differ from this version.

RESULTS

Characterization of ROS induced by glitazones in C6 glioma cells.

Our previous work has shown that glitazones generate ROS that cause glioma cell death (Perez-Ortiz *et al.*, 2004). To further investigate the mechanisms by which glitazones alter glioma cell viability we first characterized the oxidative-stress response triggered by ciglitazone, rosiglitazone and pioglitazone. Rat C6 glioma cells were loaded with the ROS-sensitive fluorescent probe H_2DCF in the absence or presence of the different glitazones. The intracellular DCF fluorescence resulting from interaction of H_2DCF with ROS was evaluated by microscopy and flow cytometry. As shown in Figure 1A, the microscopy images showed an increase in intracellular ROS 1 h after addition of each glitazone at 20 μM. Quantitative analysis of fluorescence accumulated by cells in these experiments (Figure 1B) revealed that the maximal increase was achieved by ciglitazone treatment (5.4 fold), followed by rosiglitazone (3.1 fold) and pioglitazone (1.9 fold). Flow cytometry experiments confirmed statistically significant increases in DCF fluorescence 15 min after addition of any of the glitazones at 20 μM (Figure 1C). The more robust effect was observed in the ciglitazone-treated group. All glitazones affected ROS production in a dose-dependent manner. At the lowest concentration used (10 μM), ciglitazone induced a highly significant increase in DCF fluorescence ($p<0.0001$ vs. untreated controls), pioglitazone caused a moderate change ($p<0.05$ vs. untreated controls) and rosiglitazone was ineffective.

This analysis was complemented with the measurement of $O_2^{\cdot -}$ by flow cytometry (Figure 2A). For this purpose, cells were loaded with hydroethidine (HE), treated with glitazones and processed as described for DCF detection. HE fluorescence (excitation 488 nm, emission 575 nm) increased markedly with 10 or 20 μM ciglitazone, but did not change with either rosiglitazone or pioglitazone. The specificity of HE for $O_2^{\cdot -}$ in live cells is limited by

Molecular Pharmacology Fast Forward. Published on May 15, 2007 as DOI: 10.1124/mol.106.032458
This article has not been copyedited and formatted. The final version may differ from this version.

autooxidation and other processes that can yield ethidium. However, $O_2^{\cdot -}$ has been shown to react with HE to form 2-hydroxyethidium, which can be selectively excited at 396 nm with little interference from other oxidation products (Robinson *et al.*, 2006). We used these conditions in imaging experiments, due to the lack of an appropriate laser line in our flow cytometer. As a positive control for $O_2^{\cdot -}$ formation, cells were incubated with the redox-cycling dimethoxynaphtoquinone (DMNQ). Figure 2B shows a time course of 2-hydroxyethidium formation, which occurred within minutes of ciglitazone addition. The HE oxidation was more sustained with DMNQ. These results complement the cytometric analysis and support that $O_2^{\cdot -}$ is in fact produced by ciglitazone in C6 cells. In conclusion, this first set of experiments reveals that all glitazones affect ROS production in C6 glioma cells. However, substantial differences among glitazones could be observed, ciglitazone causing higher oxidative stress than rosiglitazone or pioglitazone.

Production of ROS by glitazones: need for functional mitochondria.

It is well accepted that the mitochondrial electron transport chain is a major endogenous source of ROS (Boveris *et al.*, 1972). Generation of ROS by mitochondria depends on the mitochondrial membrane potential and its electron transport chain flux. Thus, mitochondrial ROS production was shown to decrease exponentially with decreasing $\Delta\Psi m$ (Brand *et al.*, 2004). Therefore, to evaluate the implication of mitochondria on glitazone-induced ROS we examined the effect of altering the mitochondrial membrane potential with FCCP on the ability of ciglitazone to generate ROS. FCCP is a mitochondrial uncoupling agent that acts by carrying protons across the inner mitochondrial membrane. Dissipation of the proton gradient by FCCP leads to a rapid depolarization of mitochondria, acceleration of the electron transport chain and, consequently, impairment of ROS production by the mitochondria. Therefore, FCCP is expected to inhibit ROS production induced by glitazones if the ROS

Molecular Pharmacology Fast Forward. Published on May 15, 2007 as DOI: 10.1124/mol.106.032458
This article has not been copyedited and formatted. The final version may differ from this version.

originate in mitochondria. Figure 3A shows DCF fluorescence of C6 glioma cells after 15 min incubation with 10 μM ciglitazone in the absence or presence of FCCP. Whereas 1-2 μM FCCP alone did not alter basal ROS levels, preincubation with FCCP completely inhibited ciglitazone-mediated ROS production. These observations suggest that the mitochondrial electron transport chain is the main source of ROS in C6 glioma cells treated with glitazones. In addition, the availability of energy substrates determines mitochondrial membrane potential and electron transport rate, so that impairment of mitochondria access to fuel severely dampens mitochondrial function and the capacity of mitochondria to produce ROS (Nishikawa *et al.*, 2000). Therefore, to further prove the involvement of mitochondrial electron transport chain in the oxidative stress caused by glitazones we analyzed the consequences of suppressing glucose availability. For these experiments C6 glioma cells were maintained in HBSS medium with 5.5 mM D-glucose or the non-metabolizing compound 2-deoxy-glucose. DCF fluorescence recordings after treatment with 10 μM ciglitazone during 15 minutes are shown in Figure 3B. 2-deoxy-glucose completely abrogated the ability of ciglitazone to generate ROS. Removal of D-glucose from the medium produced the same inhibition (data not shown). Moreover, similar results were also obtained using the $O_2^{\cdot -}$ probe HE (data not shown). In conclusion, these experiments further support our previous evidence indicating that the source of glitazone-induced ROS is the mitochondria.

The electron transport chain as the molecular target of glitazones in mitochondria.

Once determined that ROS synthesis by glitazones is linked to mitochondria we set up experiments to directly test the influence of glitazones on complex I of the electron transport chain. This respiratory complex is the main mitochondrial site in which ROS can be originated in mammals (Turrens, 2003). Moreover, several agents that interact with complex I are known to increase oxidative stress (Votyakova and Reynolds, 2001; Schonfeld and

Reiser, 2006). The effect of glitazones on the oxygen consumption of freshly detached C6 glioma cells was evaluated with an oxygen electrode. Permeabilized cells were energized with complex I substrates (5 mM pyruvate/2.5 mM malate) during 3 minutes, after which 250 μM ADP was added to induce state 3 of respiration for another 3 minutes. At that point, the effect of 10 μM ciglitazone, rosiglitazone or pioglitazone treatment on oxygen consumption was evaluated. Results are shown in Figure 4A as percentage of untreated controls. Ciglitazone and rosiglitazone decreased the oxygen consumption rate by approximately 27.5% and 21.5%, respectively ($p<0.01$). In turn, pioglitazone diminished respiration by 18.5% ($p<0.05$). It is interesting to note that the potency of inhibition was in accordance with the ROS level elicited by each glitazone, suggesting that ROS production can be a consequence of the glitazone inhibition of the electron transport chain.

Inhibition of complex I-dependent oxygen consumption by glitazones prompted us to further analyze the involvement of the mitochondrial electron transport chain complexes in ROS induction. Figure 4B shows the effects of different mitochondrial inhibitors on ciglitazone-evoked ROS production. C6 glioma cell cultures grown to a subconfluent density were incubated with the complex I inhibitor rotenone (Rote, 2 μM), complex III inhibitor antimycin-A (Antim, 1 μM) or the ATP synthase inhibitor oligomycin (Olig, 10 μM). These drugs were also used in combination to assess further inhibition of mitochondrial function. All inhibitors induced significant increases in $O_2^{\cdot -}$ generation when used alone or in combination in a flow cytometry assay using the probe HE. Nevertheless, addition of 10 μM ciglitazone significantly increased $O_2^{\cdot -}$ production beyond the levels achieved by each of the inhibitors alone. In conclusion, none of the inhibitors tested can reproduce the ROS-generating action of glitazones, suggesting that the molecular target of glitazones in mitochondria differs from those of the inhibitors tested. These observations are compatible

Molecular Pharmacology Fast Forward. Published on May 15, 2007 as DOI: 10.1124/mol.106.032458
This article has not been copyedited and formatted. The final version may differ from this version.

with an interaction upstream of the rotenone inhibition site in complex I, or with a multiplicity of action sites of glitazones in mitochondria.

Glitazones depolarize mitochondria and lower mitochondrial pH in C6 glioma cells.

Having shown the implication of the mitochondrial electron transport chain in ROS production induced by glitazones in C6 glioma cells, and the likely inhibition at the level of complex I, we next examined whether mitochondrial membrane potential was affected, as would be expected from the proposed mechanism of action. Mitochondrial transmembrane electric potential ($\Delta\Psi m$) was estimated by fluorescence microscopy using the probe TMRE, a small cationic molecule that accumulates in negatively charged compartments such as the mitochondrial matrix following Nernst´s equation. C6 cells were preincubated 15 minutes with 0.1 mM TMRE. Subsequent treatment with 10 μM ciglitazone provoked mitochondrial depolarization, detected in the images as a gradual loss of mitochondrial staining, accompanied by an increase in cytoplasmic, nuclear and extracellular fluorescence resulting from TMRE diffusion (Figure 5A and supplemental Figure 1). Rosiglitazone and pioglitazone also induced mitochondrial depolarization, although the effect was clearly more limited. The mitochondrial uncoupler FCCP (1 μM) was used to produce complete loss of $\Delta\Psi m$ after incubation with glitazones. Images showing TMRE fluorescence changes after addition of glitazones are shown in Figure 5A, whereas the plots depicted in Figure 5B illustrate the temporal courses of mitochondrial depolarization. In these recordings, TMRE values were expressed as the nuclear versus perinuclear fluorescence ratio. Nuclear localization of TMRE represents its diffusion from depolarizing mitochondria, while perinuclear fluorescence corresponds to polarized mitochondria plus some cytoplasmic diffuse staining. Therefore, increases in the nuclear/perinuclear fluorescence ratio indicate mitochondrial depolarization (as demonstrated in more detail in supplemental Figure 1 in a single cell) and thus provide a

Molecular Pharmacology Fast Forward. Published on May 15, 2007 as DOI: 10.1124/mol.106.032458
This article has not been copyedited and formatted. The final version may differ from this version.

reliable estimate of the ΔΨm in single cells. Control experiments with FCCP used alone showed that it depolarized mitochondria in seconds and that this effect was reversible upon washing (supplemental video). In contrast, the depolarization induced by ciglitazone was not reversed with removal of the drug from the bath in imaging experiments of up to 1 hour duration, suggesting that the mechanism of action was different from that of FCCP.

The mitochondrial proton-motive force has two constituents, membrane potential (ΔΨm) and pH gradient across the inner mitochondrial membrane (ΔpHm). We used the recombinant pH indicator "mito-EYFP H148G" (see supplemental Methods) to determine whether mitochondrial pH was affected by glitazones. Supplemental Figure 2 shows that ciglitazone (10 μM) decreased resting mitochondrial pH in C6 cells transfected with mito-EYFP H148G. The reduction of mitochondrial pH by ciglitazone occurred concomitantly with the loss of ΔΨm, as was observed in experiments combining imaging of C6 cells transfected with the pH probe and labeled with TMRE (supplemental Figure 3), which were well separated spectrally. In summary, these results evidence rapid (within minutes) and marked effects of glitazones on ΔΨm and ΔpHm in C6 glioma cells, which were more pronounced with ciglitazone. The reason for this mitochondrial impairment could be the primary block in the electron transport chain described above, or secondary damage caused by ROS being released from mitochondria. It is likely that the inhibition of the respiratory chain produces ROS, depolarization and decrease of mitochondrial ΔpH at the same time.

Extramitochondrial sources of ROS are unresponsive to ciglitazone.

The next set of experiments was designed to test whether extramitochondrial sources of ROS are also responsible for the ROS increase generated by glitazones. Cytosolic NADPH-oxidase and xanthine-oxidase were tested as possible glitazone targets using specific enzyme inhibitors. In these experiments $O_2^{\cdot -}$ was monitored by flow cytometry with the probe HE. As

Molecular Pharmacology Fast Forward. Published on May 15, 2007 as DOI: 10.1124/mol.106.032458
This article has not been copyedited and formatted. The final version may differ from this version.

shown in supplemental Figure 4, neither apocynin (20 μM) nor allopurinol (0.1 mM), inhibitors of NADPH-oxidase and xanthine-oxidase, respectively, were able to modify ciglitazone-mediated $O_2^{\cdot -}$ production. These compounds did not have any effect on HE fluorescence by themselves (data not shown). Therefore, glitazones show specificity for mitochondria as their target in relation to ROS production.

NO modulates $O_2^{\cdot -}$ production by glitazones: implications for cell survival.

As shown in Figure 1, DCF fluorescence increased after glitazone treatment, illustrating that at least part of the $O_2^{\cdot -}$ generated by these drugs is converted to H_2O_2 and/or $ONOO^-$. The interaction of $O_2^{\cdot -}$ with NO to form $ONOO^-$ is at least three times faster than $O_2^{\cdot -}$ dismutation and it has been argued that $ONOO^-$ would be the compound predominantly formed in the presence of NO (Beckman and Koppenol, 1996). To investigate this issue, we first confirmed the expression of the inducible form of nitric oxide synthase (iNOS) in C6 cells by Western blot. Levels of iNOS in unstimulated C6 cells were significant, and exceeded those found in primary astrocyte cultures (supplemental Figure 5A). Since one of the downstream effectors of NO is the soluble guanylate cyclase, which yields the second messenger cGMP, we also confirmed the presence of functional iNOS indirectly by quantifying cGMP with an enzymeimmunoassay in cell extracts. There was a 9-fold increase in the basal cGMP levels by treatment of C6 cells with tumor necrosis factor-α (TNFα) plus lipopolysaccharide (LPS), well known inducers of iNOS (supplemental Figure 5B). Changes in cGMP levels were also measured by fluorescence microscopy in single live cells using the recombinant reporter cygnet-2 (Honda *et al.*, 2001). We found that the NO donor GSNO increased cGMP within minutes of addition to the extracellular medium (data not shown).

To further investigate what $O_2^{\cdot -}$ derivatives are formed in C6 cells upon glitazone exposure and the possible influence of NO in this process, we used flow cytometry with the probe

DAF-2 to monitor NO levels after glitazone treatment. DAF-2 reacts with NO in the presence of oxygen, leading to a green fluorescent triazole compound (Nagano, 1999). Consequently, the reaction of $O_2^{\cdot -}$ with NO to yield $ONOO^-$ is expected to reduce DAF-2 fluorescence. In fact, treatment of C6 glioma cells with 10 μM ciglitazone reduced DAF-2 fluorescence significantly ($p<0.05$) (Figure 6A). This decrease in NO is in accordance with the ciglitazone-mediated $O_2^{\cdot -}$ increase previously detected with HE. Therefore, these results suggest that $O_2^{\cdot -}$ released by glitazones is, at least partly, combined with NO to form $ONOO^-$. On the contrary, rosiglitazone and pioglitazone did not affect the DAF-2 signal, in correspondence with the lack of change in $O_2^{\cdot -}$ levels observed with HE fluorescence (Figure 2A). As a positive control in these assays, C6 glioma cells were also incubated with the NO donor GSNO (500 μM), which markedly increased DAF-2 fluorescence, in agreement with the results obtained with the cGMP sensor, cygnet-2.

As a second approach to study the modulation of glitazone-evoked ROS production by NO, we checked the effect of a drop in NO on $O_2^{\cdot -}$ levels in C6 glioma cells. NO levels were reduced using the NOS inhibitor N(G)-nitro-L-arginine methyl ester (L-NAME) or 1400W, a specific inhibitor of the inducible form, iNOS. The enzymeimmunoassay for cGMP described above was used to demonstrate the ability of L-NAME and 1400W to inhibit NO release (stimulated by TNFα in combination with LPS) in our experimental model. As shown in supplemental Figure 5B, both drugs are strong inhibitors of NO production in C6 cells. In addition, flow cytometry using the probe HE was used to evaluate $O_2^{\cdot -}$. Figure 6B shows that when NO synthesis was suppressed by preincubation with NAME or 1400W, HE oxidation in cells treated with 10 μM ciglitazone was enhanced reflecting an increase in $O_2^{\cdot -}$ levels. Conversely, the oxidation of HE by $O_2^{\cdot -}$ was partially lost in the presence of the NO donor GSNO, likely due to the rapid interaction between both $O_2^{\cdot -}$ and NO, yielding $ONOO^-$. In contrast to ciglitazone, rosiglitazone was unable to modify HE fluorescence when

Molecular Pharmacology Fast Forward. Published on May 15, 2007 as DOI: 10.1124/mol.106.032458
This article has not been copyedited and formatted. The final version may differ from this version.

administered either alone or in combination with NOS-inhibitors or GSNO. Therefore, our results indicate that part of the $O_2^{\cdot -}$ generated by ciglitazone reacts with NO to form $ONOO^-$. A more direct way to demonstrate $ONOO^-$ formation was to quantify the presence of nitrotyrosine by Western blot in C6 cell protein extracts. Nitrosylated tyrosine residues were found to increase by ciglitazone treatment (Figure 6C), supporting our contention of $ONOO^-$ generation. Furthermore, the band with enhanced nitration was found to comigrate with α-tubulin (supplemental Figure 6), in agreement with other reports (Eiserich *et al.*, 1999; Zedda *et al.*, 2004). The following mechanism could explain the accumulation of nitrotyrosine in tubulin over other proteins. Cells exposed to nitric oxide-derived species may have an increased pool of nitrotyrosine, which can be selectively incorporated into the extreme C-terminus of α-tubulin by a post-translational mechanism in a reaction catalyzed by tubulin-tyrosine ligase (Eiserich *et al.*, 1999; Zedda *et al.*, 2004). Therefore, enhanced tubulin tyrosine nitrosylation in ciglitazone-treated C6 cells is likely due to increased exposure to NO and funneling of the modified aminoacid into this protein.

Although it is not a free radical, $ONOO^-$ is a potent oxidant that can potentially attack a wide range of biological molecules, causing lipid peroxidation, protein oxidation and nitration (as shown above), and induction of DNA strand breaks (Salgo *et al.*, 1995). $ONOO^-$ also may impair the function of mitochondrial complex I (Riobo *et al.*, 2001), which would be in accordance with the observed reduction in oxygen consumption with complex I substrates in the presence of ciglitazone. Therefore, to elucidate whether $O_2^{\cdot -}$ conversion to $ONOO^-$ by combination with NO affects cytotoxicity of glitazones in C6 glioma cells, the effect of NOS inhibition on cell viability was tested using propidium iodide (PI) staining of cells in a flow cytometry assay. The percentage of PI-positive cells increased as soon as 3 hours after ciglitazone addition (Fig 7). This effect was partly prevented by preincubation of cells with the NOS inhibitors L-NAME and 1400W, suggesting that $ONOO^-$ contributes to ciglitazone

Molecular Pharmacology Fast Forward. Published on May 15, 2007 as DOI: 10.1124/mol.106.032458
This article has not been copyedited and formatted. The final version may differ from this version.

cytotoxicity. In conclusion, these results indicate that the fate of glioma cells treated with glitazones is affected by both $O_2^{\cdot -}$ and NO derived reactive species.

Molecular Pharmacology Fast Forward. Published on May 15, 2007 as DOI: 10.1124/mol.106.032458
This article has not been copyedited and formatted. The final version may differ from this version.

DISCUSSION

We use several strategies to identify the intracellular sources of ROS that are produced by glitazones in C6 glioma cells. The fluorescent probe H_2DCF is mainly sensitive to H_2O_2 and $ONOO^-$ (Hempel *et al.*, 1999) whereas HE detects more specifically $O_2^{\cdot -}$ (Rothe and Valet, 1990), particularly with a recent modification to the method (Robinson *et al.*, 2006), thus providing complementary information on the nature of the oxygen species released. Ciglitazone enhanced fluorescence of both probes, whereas rosiglitazone and pioglitazone had only a significant effect on H_2DCF. Our interpretation is that ciglitazone increases HE fluorescence as a consequence of the higher levels of $O_2^{\cdot -}$ produced, while rosiglitazone and pioglitazone would produce $O_2^{\cdot -}$ at a slower rate. $O_2^{\cdot -}$ may also be undetected if it is rapidly converted into H_2O_2 and/or $ONOO^-$. H_2DCF detects the latter species formed after treatment with ciglitazone, rosiglitazone or pioglitazone. The fact that the glitazone-induced ROS increase was prevented by the uncoupler FCCP and by the non-metabolizable 2-deoxy-glucose suggests that it is dependent on mitochondrial electron transport. As discussed below, glitazones may cause an inhibition of respiratory activity with substrates of complex I with two effects: one-electron transfer to O_2, with $O_2^{\cdot -}$ formation, and a drop in the $\Delta\Psi m$ and mitochondrial pH. On the other hand, our studies with inhibitors of NADPH-oxidase and xanthine-oxidase rule out these extra-mitochondrial sources of ROS. Moreover, the mechanism is likely independent of PPARγ activation, as we (Perez-Ortiz *et al.*, 2004) and others (Brunmair *et al.*, 2004) suggested for several actions of glitazones.

All glitazones tested caused mitochondrial depolarization (ciglitazone being the most potent) measured by changes in TMRE fluorescence and subcellular distribution, and a simultaneous decrease in the mitochondrial pH, determined with the novel recombinant pH indicator mito-EYFP H148G. Such a rapid drop in the mitochondrial membrane potential has also been

reported after treatment of liver HepG2 cells with troglitazone (Bova *et al.*, 2005), troglitazone or ciglitazone in mice liver mitochondria (Masubuchi *et al.*, 2006) and ciglitazone in Jurkat, Raji and human multiple myeloma cells (Kanunfre *et al.*, 2004; Ray *et al.*, 2004). Mitochondrial depolarization by glitazones could be a consequence of the opening of the mitochondrial permeability transition pore, since this mechanism has been proposed to explain the *in vitro* cytotoxicity of some glitazones (Masubuchi *et al.*, 2006). However, the mitochondrial pore inhibitor cyclosporin A did not block the glitazone-induced depolarization in our case (results not shown). Since glitazones and FCCP cause mitochondrial depolarization, it is possible that they act as uncoupling agents similar to FCCP, which accelerates the electron transport by reducing the proton gradient. However, FCCP was unable to increase ROS levels in our experiments. In consequence, glitazones are likely to induce mitochondrial depolarization, decrease in the mitochondrial pH gradient and ROS production in C6 cells by inhibiting electron transport rather than accelerating it. Other authors have proposed a direct interaction of glitazones with components of the electron transport chain, impairing the mitochondrial function. The highly lipophilic structure of glitazones would favour their accumulation in mitochondrial membranes (Brunmair *et al.*, 2004).

Our results showing that ciglitazone, rosiglitazone and pioglitazone reduce pyruvate and malate-dependent oxygen consumption in state 3 of respiration constitute a direct evidence of their inhibitory effect on mitochondrial function, involving respiratory complex I. Studies performed in muscle and liver homogenates and human cell lines support this contention and also point to complex I as the site inhibited by glitazones (Brunmair *et al.*, 2004; Scatena *et al.*, 2004). Therefore, ROS release, mitochondrial depolarization and pH drop, and inhibition of oxygen consumption elicited by glitazones are likely caused by the inhibition of mitochondrial electron transport. A similar relationship has been proposed

Molecular Pharmacology Fast Forward. Published on May 15, 2007 as DOI: 10.1124/mol.106.032458
This article has not been copyedited and formatted. The final version may differ from this version.

previously for rotenone (Li *et al.*, 2003). We observed a correlation between the inhibition of mitochondrial oxygen consumption by individual glitazones and the magnitude of the ROS burst produced, ciglitazone having the largest effect. $O_2^{\cdot -}$ and other oxygen derivatives have been shown to block the function of several respiratory complexes (Riobo *et al.*, 2001). Therefore, a positive feedback loop might be at play, in which ROS formed as a consequence of glitazone binding to mitochondria and inhibition of electron flow in complex I would enhance further ROS release.

ROS production by ciglitazone could not be blocked by any of the specific mitochondrial complex inhibitors used, including rotenone. A possible explanation is that ciglitazone inhibits electron transport upstream of the inhibition site of rotenone on complex I. Likely targets would be the flavin components of this complex, univalent electron carriers of sufficiently low redox potential to react with O_2 and produce $O_2^{\cdot -}$ when they are reduced (Massey, 1994). ROS release by those components has been implicated in a rotenone model of Parkinson (Panov *et al.*, 2005). Alternatively, the lack of effect of respiratory complex inhibitors on the induction of ROS by glitazones might be a consequence of the existence of multiple mitochondrial targets. A novel glitazone binding site in mitochondria has been demonstrated using tritiated pioglitazone and a photoaffinity crosslinker (Colca *et al.*, 2004). The protein identified, termed "mitoNEET", is located in the mitochondrial fraction of rodent brain, liver and skeletal muscle. Part of the stimulatory effect of glitazones on ROS may also be due to a feed-forward loop in which ROS further interact with several mitochondrial loci. Significantly, $O_2^{\cdot -}$ and other ROS show a well-defined affinity for the iron-sulfur clusters present at least in respiratory complexes I and II (Flint *et al.*, 1993; Riobo *et al.*, 2001). Moreover, $ONOO^-$ has the ability to inactivate several enzymes by stimulating tyrosine nitration and may cause damage to the electron transport chain (Riobo *et al.*, 2001). We observed increased nitrotyrosine in glitazone treated cells by Western blot.

We have shown that ciglitazone and rosiglitazone are lethal for human and rodent glioma cell lines, but not for primary astrocytes in culture (Perez-Ortiz *et al.*, 2004). Pioglitazone has also shown selective inhibition of glioma growth *in vivo* (Grommes et al, 2006). Tumor cells are metabolically more active (Warburg effect) and subjected to a greater oxidative stress than non-tumor astrocytes, which may explain their higher sensitivity to ROS-inducing stimuli such as glitazones. The mitochondrial mechanisms triggered by glitazones may inspire the development of new strategies for the treatment of tumors (Kondo *et al.*, 2001). In fact, several anti-tumoral agents, such as anthracyclines, cisplatin, bleomycin, arsenic trioxide and irradiation, show cytotoxicity based at least partly in the potentiation of ROS release (Pelicano *et al.*, 2004).

Our previous work established that the enhancement of ROS production by glitazones is linked to cytotoxicity in C6 glioma cells (Perez-Ortiz *et al.*, 2004). In the present study we detect $O_2^{\cdot -}$ as the initial oxygen by-product stimulated by glitazones. However, $O_2^{\cdot -}$ is rapidly metabolized into H_2O_2 and/or $ONOO^-$, which are relatively stable oxidants with the capacity to pass cell membranes and induce cell damage. Since their cytotoxicity seems to be cell-type dependent, we devoted to determine which of these $O_2^{\cdot -}$ derivatives were formed in C6 cells after glitazone treatment and their relative contribution to cytotoxicity. Mechanistically, the interaction between NO and $O_2^{\cdot -}$ to form $ONOO^-$ is favoured over the $O_2^{\cdot -}$ dismutation that results in H_2O_2 (Beckman and Koppenol, 1996). NO is the product of several cytoplasmic NO synthases (NOS), and a mitochondrial NOS isoform has also been reported (Riobo *et al.*, 2002). C6 glioma cells have been shown to possess all cytosolic NOS isoforms (Barna *et al.*, 1996; Ciampa *et al.*, 2005; Yin *et al.*, 2001) and we show the presence of iNOS by Western and functional analysis (cGMP levels).

Our results suggest that C6 glioma cells release NO that combines with $O_2^{\cdot -}$ to form $ONOO^-$, and that reactive species derived from both $O_2^{\cdot -}$ and NO are implicated in

Molecular Pharmacology Fast Forward. Published on May 15, 2007 as DOI: 10.1124/mol.106.032458
This article has not been copyedited and formatted. The final version may differ from this version.

ciglitazone cytotoxicity. Upcoming therapeutic anti-tumoral strategies might derive from this and other work on glitazones. Furthermore, the present results lead us to subscribe to an appealing proposal (Brunmair *et al.*, 2004) in which the decline in the mitochondrial function provoked by glitazones in several tissues may contribute to their antidiabetic effects, whose molecular mechanisms are still poorly characterized.

Molecular Pharmacology Fast Forward. Published on May 15, 2007 as DOI: 10.1124/mol.106.032458
This article has not been copyedited and formatted. The final version may differ from this version.

ACKNOWLEDGEMENTS

We gratefully acknowledge Ana M. Alonso for useful technical support, Dr. Laura Contreras for help with the oxygen consumption experiments, Dr. Joaquín Jordán for access to the oxygen electrode and Dr. Jorgina Satrústegui for helpful discussion and careful reading of the manuscript.

REFERENCES

Barna M, Komatsu T and Reiss C S (1996) Activation of Type III Nitric Oxide Synthase in Astrocytes Following a Neurotropic Viral Infection. *Virology* **223**:331-343.

Beckman JS and Koppenol W H (1996) Nitric Oxide, Superoxide, and Peroxynitrite: the Good, the Bad, and Ugly. *Am J Physiol* **271**:C1424-C1437.

Bova MP, Tam D, McMahon G and Mattson M N (2005) Troglitazone Induces a Rapid Drop of Mitochondrial Membrane Potential in Liver HepG2 Cells. *Toxicol Lett* **155**:41-50.

Boveris A, Oshino N and Chance B (1972) The Cellular Production of Hydrogen Peroxide. *Biochem J* **128**:617-630.

Brand MD, Affourtit C, Esteves T C, Green K, Lambert A J, Miwa S, Pakay J L and Parker N (2004) Mitochondrial Superoxide: Production, Biological Effects, and Activation of Uncoupling Proteins. *Free Radic Biol Med* **37**:755-767.

Brunmair B, Staniek K, Gras F, Scharf N, Althaym A, Clara R, Roden M, Gnaiger E, Nohl H, Waldhausl W and Furnsinn C (2004) Thiazolidinediones, Like Metformin, Inhibit Respiratory Complex I: a Common Mechanism Contributing to Their Antidiabetic Actions? *Diabetes* **53**:1052-1059.

Ciampa AR, de Prati A C, Amelio E, Cavalieri E, Persichini T, Colasanti M, Musci G, Marlinghaus E, Suzuki H and Mariotto S (2005) Nitric Oxide Mediates Anti-Inflammatory Action of Extracorporeal Shock Waves. *FEBS Lett* **579**:6839-6845.

Colca JR, McDonald W G, Waldon D J, Leone J W, Lull J M, Bannow C A, Lund E T and Mathews W R (2004) Identification of a Novel Mitochondrial Protein ("MitoNEET") Cross-Linked Specifically by a Thiazolidinedione Photoprobe. *Am J Physiol Endocrinol Metab* **286**:E252-E260.

Delerive P, Fruchart J C and Staels B (2001) Peroxisome Proliferator-Activated Receptors in Inflammation Control. *J Endocrinol* **169**:453-459.

Eiserich JP, Estevez A G, Bamberg T V, Ye Y Z, Chumley P H, Beckman J S and Freeman B A (1999) Microtubule Dysfunction by Posttranslational Nitrotyrosination of Alpha-Tubulin: a Nitric Oxide-Dependent Mechanism of Cellular Injury. *Proc Natl Acad Sci U S A* **96**:6365-6370.

Feinstein DL, Spagnolo A, Akar C, Weinberg G, Murphy P, Gavrilyuk V and Dello R C (2005) Receptor-Independent Actions of PPAR Thiazolidinedione Agonists: Is Mitochondrial Function the Key? *Biochem Pharmacol* **70**:177-188.

Flint DH, Tuminello J F and Emptage M H (1993) The Inactivation of Fe-S Cluster Containing Hydro-Lyases by Superoxide. *J Biol Chem* **268**:22369-22376.

Grommes C, Landreth G E and Heneka M T (2004) Antineoplastic Effects of Peroxisome Proliferator-Activated Receptor Gamma Agonists. *Lancet Oncol* **5**:419-429.

Hempel SL, Buettner G R, O'Malley Y Q, Wessels D A and Flaherty D M (1999) Dihydrofluorescein Diacetate Is Superior for Detecting Intracellular Oxidants: Comparison With 2',7'-Dichlorodihydrofluorescein Diacetate, 5(and 6)-Carboxy-2',7'-

Dichlorodihydrofluorescein Diacetate, and Dihydrorhodamine 123. *Free Radic Biol Med* **27**:146-159.

Honda A, Adams S R, Sawyer C L, Lev-Ram V, Tsien R Y and Dostmann W R (2001) Spatiotemporal Dynamics of Guanosine 3',5'-Cyclic Monophosphate Revealed by a Genetically Encoded, Fluorescent Indicator. *Proc Natl Acad Sci U S A* **98**:2437-2442.

Kanunfre CC, da Silva Freitas J J, Pompeia C, Goncalves d A, Cury-Boaventura M F, Verlengia R and Curi R (2004) Ciglitizone and 15d PGJ2 Induce Apoptosis in Jurkat and Raji Cells. *Int Immunopharmacol* **4**:1171-1185.

Kondo M, Oya-Ito T, Kumagai T, Osawa T and Uchida K (2001) Cyclopentenone Prostaglandins As Potential Inducers of Intracellular Oxidative Stress. *J Biol Chem* **276**:12076-12083.

Li N, Ragheb K, Lawler G, Sturgis J, Rajwa B, Melendez J A and Robinson J P (2003) Mitochondrial Complex I Inhibitor Rotenone Induces Apoptosis Through Enhancing Mitochondrial Reactive Oxygen Species Production. *J Biol Chem* **278**:8516-8525.

Massey V (1994) Activation of Molecular Oxygen by Flavins and Flavoproteins. *J Biol Chem* **269**:22459-22462.

Masubuchi Y, Kano S and Horie T (2006) Mitochondrial Permeability Transition As a Potential Determinant of Hepatotoxicity of Antidiabetic Thiazolidinediones. *Toxicology* **222**:233-239.

Nagano T (1999) Practical Methods for Detection of Nitric Oxide. *Luminescence* **14**:283-290.

Narayanan PK, Hart T, Elcock F, Zhang C, Hahn L, McFarland D, Schwartz L, Morgan D G and Bugelski P (2003) Troglitazone-Induced Intracellular Oxidative Stress in Rat Hepatoma Cells: a Flow Cytometric Assessment. *Cytometry A* **52**:28-35.

Nishikawa T, Edelstein D, Du X L, Yamagishi S, Matsumura T, Kaneda Y, Yorek M A, Beebe D, Oates P J, Hammes H P, Giardino I and Brownlee M (2000) Normalizing Mitochondrial Superoxide Production Blocks Three Pathways of Hyperglycaemic Damage. *Nature* **404**:787-790.

Panov A, Dikalov S, Shalbuyeva N, Taylor G, Sherer T and Greenamyre J T (2005) Rotenone Model of Parkinson Disease: Multiple Brain Mitochondria Dysfunctions After Short Term Systemic Rotenone Intoxication. *J Biol Chem* **280**:42026-42035.

Pelicano H, Carney D and Huang P (2004) ROS Stress in Cancer Cells and Therapeutic Implications. *Drug Resist Updat* **7**:97-110.

Perez-Ortiz JM, Tranque P, Vaquero C F, Domingo B, Molina F, Calvo S, Jordan J, Cena V and Llopis J (2004) Glitazones Differentially Regulate Primary Astrocyte and Glioma Cell Survival. Involvement of Reactive Oxygen Species and Peroxisome Proliferator-Activated Receptor-Gamma. *J Biol Chem* **279**:8976-8985.

Radi R, Cassina A and Hodara R (2002) Nitric Oxide and Peroxynitrite Interactions With Mitochondria. *Biol Chem* **383**:401-409.

Ray DM, Bernstein S H and Phipps R P (2004) Human Multiple Myeloma Cells Express Peroxisome Proliferator-Activated Receptor Gamma and Undergo Apoptosis Upon Exposure to PPARgamma Ligands. *Clin Immunol* **113**:203-213.

Riobo NA, Clementi E, Melani M, Boveris A, Cadenas E, Moncada S and Poderoso J J (2001) Nitric Oxide Inhibits Mitochondrial NADH:Ubiquinone Reductase Activity Through Peroxynitrite Formation. *Biochem J* **359**:139-145.

Riobo NA, Melani M, Sanjuan N, Fiszman M L, Gravielle M C, Carreras M C, Cadenas E and Poderoso J J (2002) The Modulation of Mitochondrial Nitric-Oxide Synthase Activity in Rat Brain Development. *J Biol Chem* **277**:42447-42455.

Robinson KM, Janes M S, Pehar M, Monette J S, Ross M F, Hagen T M, Murphy M P and Beckman J S (2006) Selective Fluorescent Imaging of Superoxide in Vivo Using Ethidium-Based Probes. *Proc Natl Acad Sci U S A* **103**:15038-15043.

Rothe G and Valet G (1990) Flow Cytometric Analysis of Respiratory Burst Activity in Phagocytes With Hydroethidine and 2',7'-Dichlorofluorescin. *J Leukoc Biol* **47**:440-448.

Salgo MG, Bermudez E, Squadrito G L and Pryor W A (1995) Peroxynitrite Causes DNA Damage and Oxidation of Thiols in Rat Thymocytes [Corrected]. *Arch Biochem Biophys* **322**:500-505.

Scatena R, Bottoni P, Martorana G E, Ferrari F, De S P, Rossi C and Giardina B (2004) Mitochondrial Respiratory Chain Dysfunction, a Non-Receptor-Mediated Effect of

Synthetic PPAR-Ligands: Biochemical and Pharmacological Implications. *Biochem Biophys Res Commun* **319**:967-973.

Schonfeld P and Reiser G (2006) Rotenone-Like Action of the Branched-Chain Phytanic Acid Induces Oxidative Stress in Mitochondria. *J Biol Chem* **281**:7136-7142.

Turrens JF (2003) Mitochondrial Formation of Reactive Oxygen Species. *J Physiol* **552**:335-344.

Votyakova TV and Reynolds I J (2001) DeltaPsi(m)-Dependent and -Independent Production of Reactive Oxygen Species by Rat Brain Mitochondria. *J Neurochem* **79**:266-277.

Yin JH, Yang D I, Chou H, Thompson E M, Xu J and Hsu C Y (2001) Inducible Nitric Oxide Synthase Neutralizes Carbamoylating Potential of 1,3-Bis(2-Chloroethyl)-1-Nitrosourea in C6 Glioma Cells. *J Pharmacol Exp Ther* **297**:308-315.

Yki-Jarvinen H (2004) Thiazolidinediones. *N Engl J Med* **351**:1106-1118.

Zedda M, Lepore G, Gadau S, Manca P and Farina V (2004) Morphological and Functional Changes Induced by the Amino Acid Analogue 3-Nitrotyrosine in Mouse Neuroblastoma and Rat Glioma Cell Lines. *Neurosci Lett* **363**:190-193.

Molecular Pharmacology Fast Forward. Published on May 15, 2007 as DOI: 10.1124/mol.106.032458
This article has not been copyedited and formatted. The final version may differ from this version.

FOOTNOTES

J.M.P.O. is a fellow from Consejería de Sanidad, Junta de Comunidades de Castilla-La Mancha, Spain (Ref. 2006-BIN-1383). This work was supported by grants from Consejería de Sanidad, JCCM, Spain (Refs. 04007-00 and GC04-005) to J.L.

Molecular Pharmacology Fast Forward. Published on May 15, 2007 as DOI: 10.1124/mol.106.032458
This article has not been copyedited and formatted. The final version may differ from this version.

FIGURE LEGENDS

Figure 1 ROS detection by DCF fluorescence

A, fluorescence microscopy of C6 glioma cells loaded with H_2DCF-DA. Images show the initial DCF fluorescence (control, left panels), and after a 1 h treatment with 20 μM ciglitazone, rosiglitazone or pioglitazone (right panels). Higher fluorescence intensities correspond with higher levels of ROS production. **B**, quantitation of DCF fluorescence in microscopic images. Intracellular fluorescence values were averaged after background subtraction. **C**, C6 glioma cells were incubated 15 min with 10 or 20 μM ciglitazone, rosiglitazone or pioglitazone in the presence of 2.5 μM H_2DCF, and fluorescence intensity was evaluated by flow cytometry. Results represent mean ± S.D., and are expressed as percentage of controls. Statistical significance of glitazone-treated groups vs. untreated controls is indicated ($^{\#}$, $p<0.05$; *, $p<0.01$; ***, $p<0.0001$).

Figure 2 ROS detection by HE fluorescence

A, C6 glioma cells were incubated for 15 min with 10 or 20 μM ciglitazone, rosiglitazone or pioglitazone in the presence of 5 μM HE and fluorescence intensity was evaluated by flow cytometry. Mean values are expressed as percentage of fluorescence of untreated controls. Statistical significance of glitazone-treated groups vs. respective controls is indicated (***, $p<0.0001$). **B**, time course of HE fluorescence in imaging experiments using excitation at 397 nm and emission at 595 nm on a widefield microscope. C6 cells were treated with 20 μM ciglitazone or DMNQ at time=10 min (arrow). Regions were manually drawn over cells and fluorescence change over time is expressed as F/F_0 (fluorescence at each time point/initial fluorescence). The mean of 27 cells from 3 independent experiments (ciglitazone) and 40 cells from 4 experiments (DMNQ) are shown.

Molecular Pharmacology Fast Forward. Published on May 15, 2007 as DOI: 10.1124/mol.106.032458
This article has not been copyedited and formatted. The final version may differ from this version.

Figure 3 Influence of mitochondrial electron transport on ROS induction by glitazones

A, DCF fluorescence of C6 glioma cells incubated during 15 min with 10 μM ciglitazone or vehicle (control) was analyzed in the presence of 0, 1 and 2 μM of the uncoupling agent FCCP by flow cytometry. Results represent means and are expressed as percentage of untreated cells in the absence of FCCP. This agent completely inhibits the ciglitazone-mediated ROS production, illustrating the dependency of glitazone-induced ROS production on mitochondrial polarity and rate of electron transport. **B**, DCF fluorescence was examined in C6 glioma cultures after a 15 min treatment with 10 μM ciglitazone or vehicle by flow cytometry. Cells were maintained in HBSS medium with 5.5 mM of either D-glucose or the non-metabolizing glucose analogue 2-deoxy-glucose. Data are presented as percentage of D-glucose controls, and are expressed as mean ± S.D. Asterisks indicate statistical significance of differences respect to untreated controls (***, $p<0.0001$). Ciglitazone is unable to generate ROS in the absence of D-glucose suggesting that mitochondria are the main ROS-generating source.

Figure 4 Effect of glitazones on state 3 of respiration and mitochondrial electron transport chain inhibitors on ciglitazone-induced $O_2^{\cdot -}$ production

A, C6 glioma cells (10^7) freshly detached in 1 ml of standard medium were permeabilized with 40 μM digitonin and immediately used to monitor oxygen consumption. Mitochondria were energized with 5 mM pyruvate/2.5 mM malate (complex I substrates), and ADP (250 μM) was used to induce state 3 of respiration. Ciglitazone, rosiglitazone, pioglitazone (10 μM for all) or vehicle were added to the reaction chamber 3 min after ADP. Results represent mean ± S.D. of oxygen consumption, and are expressed as percentage of untreated controls ($^{\#}$, $p<0.05$; *, $p < 0.01$). All glitazones inhibit complex I-dependent state 3 of respiration. **B**,

Molecular Pharmacology Fast Forward. Published on May 15, 2007 as DOI: 10.1124/mol.106.032458
This article has not been copyedited and formatted. The final version may differ from this version.

C6 glioma cells were incubated for 15 min with 10 μM ciglitazone or vehicle in the presence of 2 μM rotenone (rote), 10 μM oligomycin (olig) and/or 1 μM antimycin-A (antim) as indicated. $O_2^{\cdot -}$ production was evaluated by flow cytometry after addition of the fluorescent probe hydroethidine (5 μM) to cell cultures 5 min prior initiation of glitazone treatment. Data shown are expressed as percentage of untreated controls. Statistical significance of ciglitazone-treated groups vs. respective controls is shown ($^{\#}$, $p<0.05$; *, $p < 0.01$; **, $p < 0.001$). None of the mitochondrial inhibitors used, alone or in combination, was able to abolish $O_2^{\cdot -}$ production induced by ciglitazone.

Figure 5 Temporal courses of mitochondrial depolarization by glitazones

A, fluorescence microscopy images of C6 glioma cells showing the initial TMRE fluorescence state in vehicle-treated controls (left panels), after 10 μM ciglitazone, rosiglitazone or pioglitazone treatment (middle panels), and following addition of 1 μM FCCP (right panels). FCCP is herein used as a positive control of mitochondrial depolarization, yielding the maximal fluorescence shift. This is observed as diffusion of staining from the mitochondria to the nucleus and cytosol. **B,** time course of mitochondrial depolarization after glitazone and FCCP treatments. Results are expressed as mean ± S.D. of the ratio between nuclear and perinuclear fluorescence. Although all glitazones tested induce mitochondrial depolarization, the greatest effect was obtained with ciglitazone.

Figure 6 Interaction between $O_2^{\cdot -}$ and NO in C6 cells treated with glitazones

A, C6 glioma cells were incubated with 10 μM ciglitazone, rosiglitazone or pioglitazone during 15 min, whereas controls were treated with vehicle (0.02% Me_2SO) or the NO donor GSNO (500 μM). DAF-2 fluorescence, representing NO production, was evaluated by flow cytometry. **B**, flow cytometry analysis of HE fluorescence induced by a 15 min exposure to

Molecular Pharmacology Fast Forward. Published on May 15, 2007 as DOI: 10.1124/mol.106.032458
This article has not been copyedited and formatted. The final version may differ from this version.

10 μM ciglitazone or rosiglitazone. In addition, cells were pre-incubated for 2 h with a NOS inhibitor (500 μM L-NAME or 50 μM 1400W), or with 500 μM GSNO. **C**, C6 cells were treated for 3 h with 20 μM ciglitazone or vehicle, and proteins were extracted for nitrotyrosine detection by Western blotting. Densitometric analysis of nitrotyrosine immunoblots is also shown. In all panels, results are expressed as percentage of controls treated with the appropriate vehicle. Data are presented as mean ± S.D. and statistically significant changes are indicated ($^{\#}$, $p<0.05$; *, $p < 0.01$; ***, $p<0.0001$).

Figure 7 Effect of NOS inhibitors on cell survival

C6 cells were stimulated for 3 h with 20 μM ciglitazone after a 2 h incubation with 500 μM L-NAME, 50 μM 1400W, or vehicle (Me_2SO). Viability was examined by flow cytometry after 10 min exposure to PI (10 μg/ml). Results represent percentage of PI-positive cells and are expressed as mean ± S.D. Statistical significance of ciglitazone-treated cells vs. respective controls is shown (**, $p < 0.001$).

Figure 1

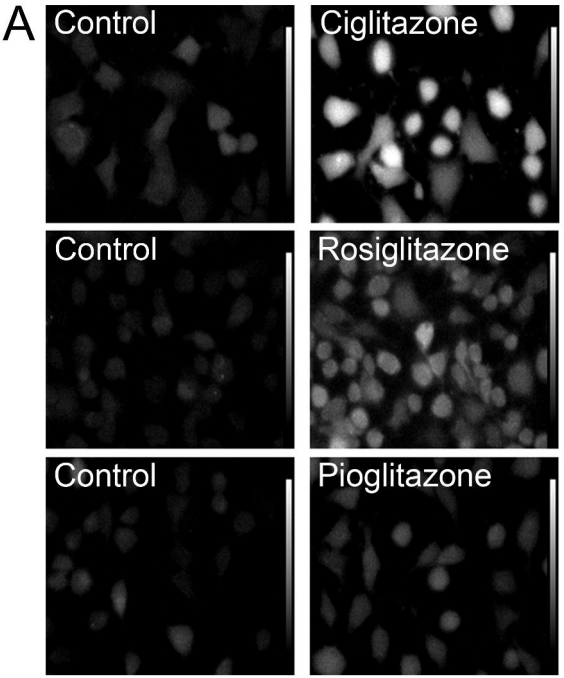
A
Control
Ciglitazone
Control
Rosiglitazone
Control
Pioglitazone

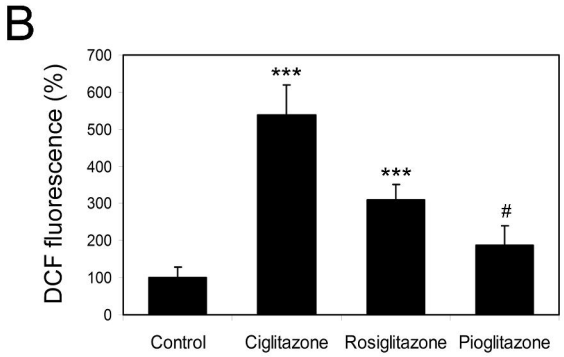
B
DCF fluorescence (%)
700
600
500
400
300
200
100
0
***
***
#
Control
Ciglitazone
Rosiglitazone
Pioglitazone

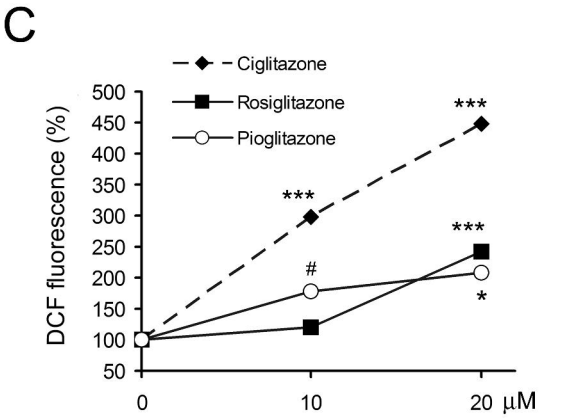
C
Ciglitazone
Rosiglitazone
Pioglitazone
DCF fluorescence (%)
500
450
400
350
300
250
200
150
100
50
***
***
***
#
*
0
10
20 μM

Figure 2

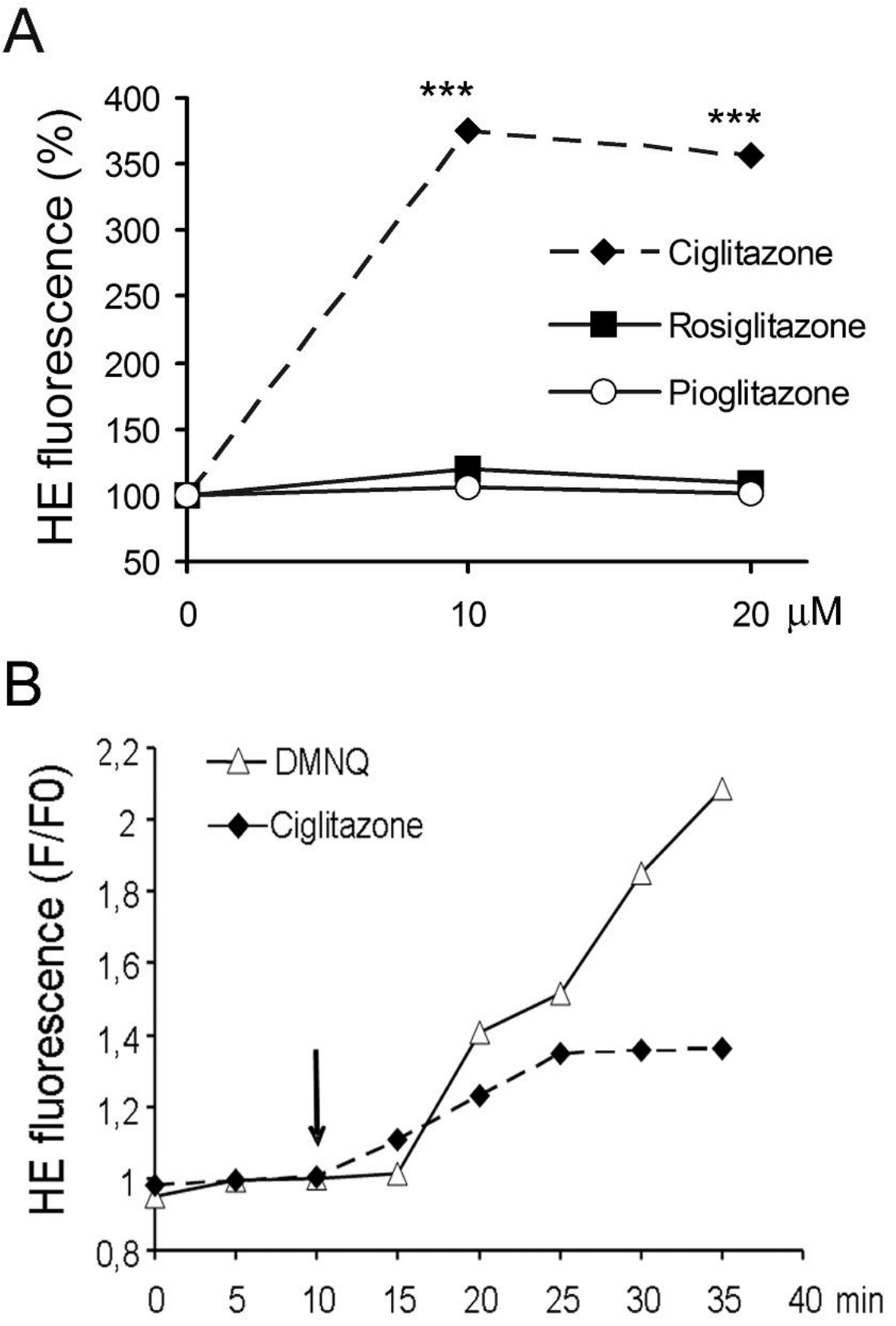
A
HE fluorescence (%)
400
350
300
250
200
150
100
50
***
***
Ciglitazone
Rosiglitazone
Pioglitazone
0
10
20 µM
B
HE fluorescence (F/F0)
2,2
2
1,8
1,6
1,4
1,2
1
0,8
DMNQ
Ciglitazone
0
5
10
15
20
25
30
35
40 min

Figure 3

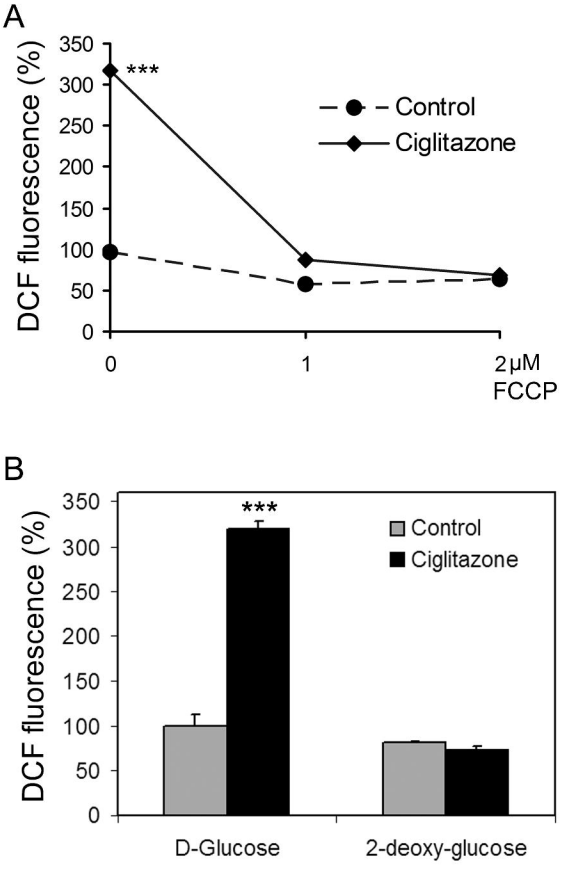
A
DCF fluorescence (%)
350
300
250
200
150
100
50
0
***
Control
Ciglitazone
0
1
2μM
FCCP
B
DCF fluorescence (%)
350
300
250
200
150
100
50
0
***
Control
Ciglitazone
D-Glucose
2-deoxy-glucose

Figure 4

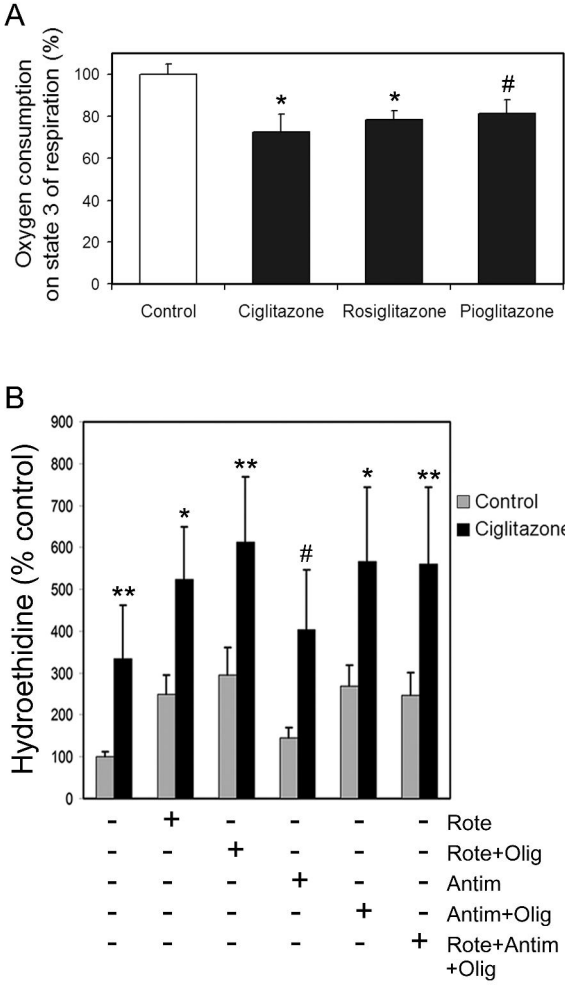
A
Oxygen consumption on state 3 of respiration (%)
100
80
60
40
20
0
*
*
#
Control
Ciglitazone
Rosiglitazone
Pioglitazone
B
Hydroethidine (% control)
900
800
700
600
500
400
300
200
100
0
**
*
**
#
*
**
Control
Ciglitazone
- + - - - - Rote
- - + - - - Rote+Olig
- - - + - - Antim
- - - - + - Antim+Olig
- - - - - + Rote+Antim +Olig

Figure 5

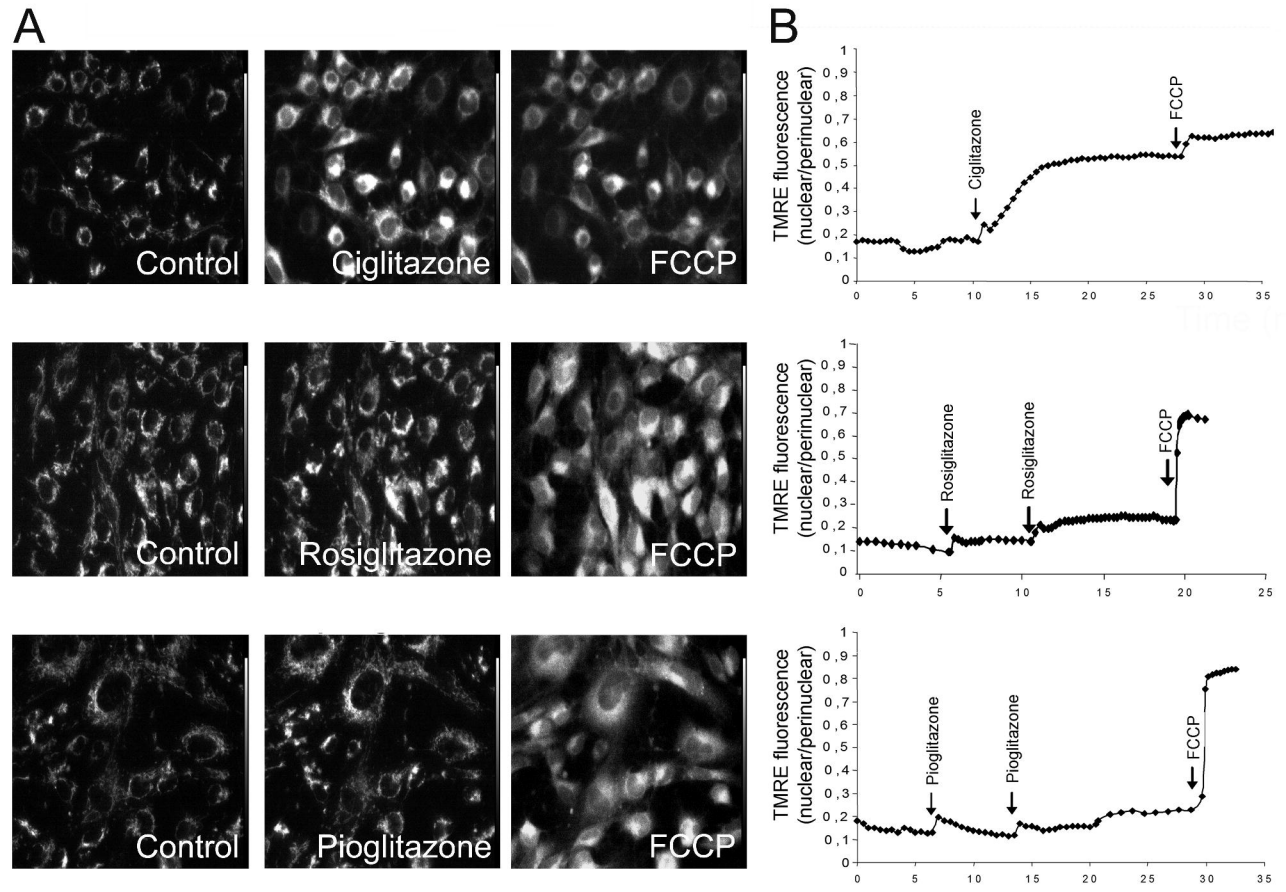
A
Control
Ciglitazone
FCCP
Control
Rosiglitazone
FCCP
Control
Pioglitazone
FCCP
B
TMRE fluorescence (nuclear/perinuclear)
Ciglitazone
FCCP
Rosiglitazone
Rosiglitazone
FCCP
Pioglitazone
Pioglitazone
FCCP

Figure 6

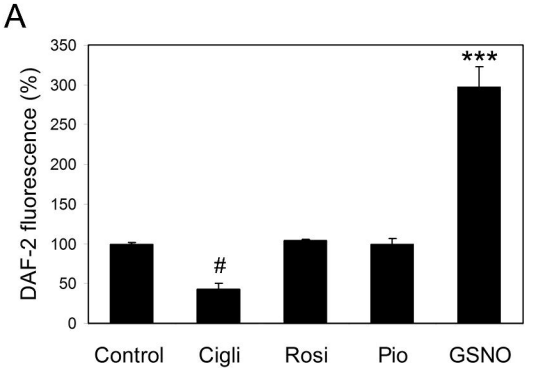
A
DAF-2 fluorescence (%)
350
300
250
200
150
100
50
0
***
#
Control
Cigli
Rosi
Pio
GSNO

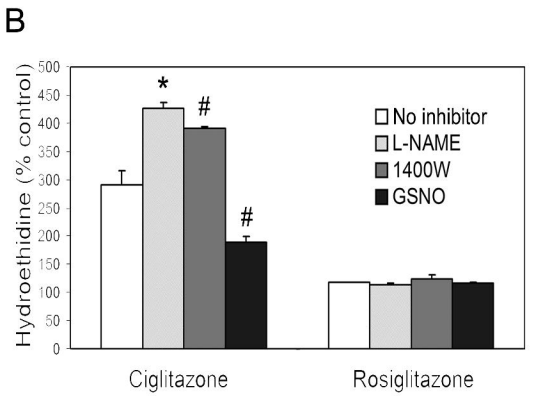
B
Hydroethidine (% control)
500
450
400
350
300
250
200
150
100
50
0
*
#
#
No inhibitor
L-NAME
1400W
GSNO
Ciglitazone
Rosiglitazone

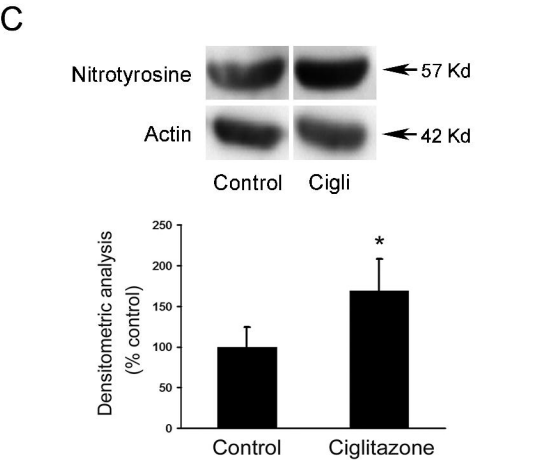
C
Nitrotyrosine
57 Kd
Actin
42 Kd
Control
Cigli
Densitometric analysis
(% control)
250
200
150
100
50
0
*
Control
Ciglitazone

Figure 7

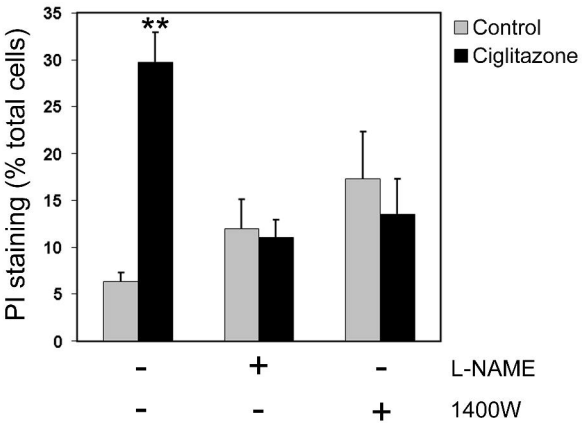
PI staining (% total cells)
35
30
25
20
15
10
5
0
**
Control
Ciglitazone
-
+
-
L-NAME
-
-
+
1400W

Supplemental Figure 1

A

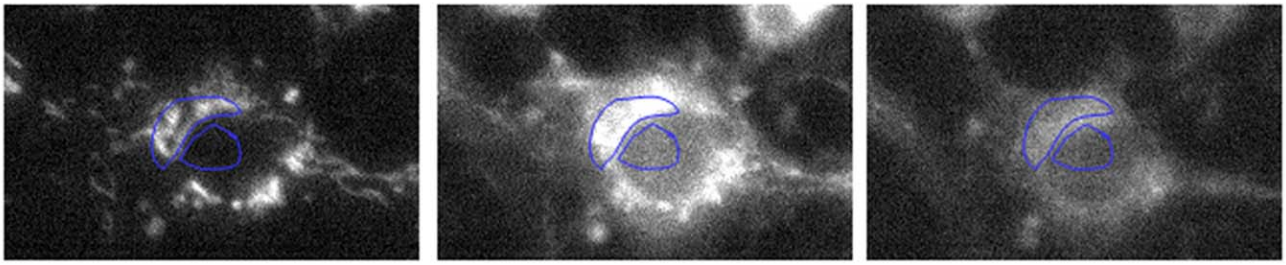

Control (min 9) Ciglitazone (min 16) FCCP (min 36)

B

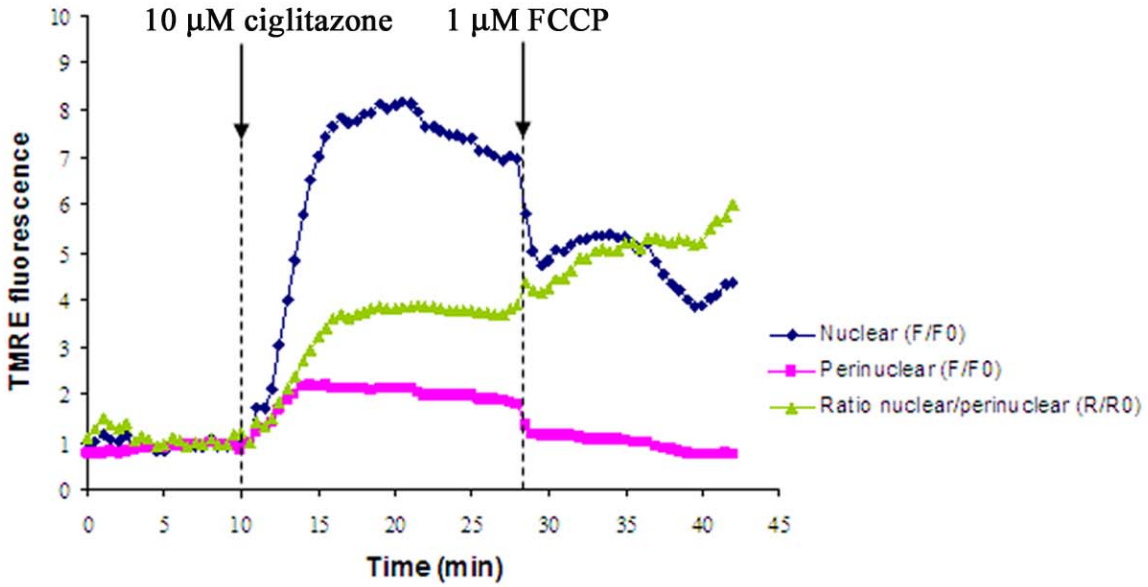

Supplemental Figure 2

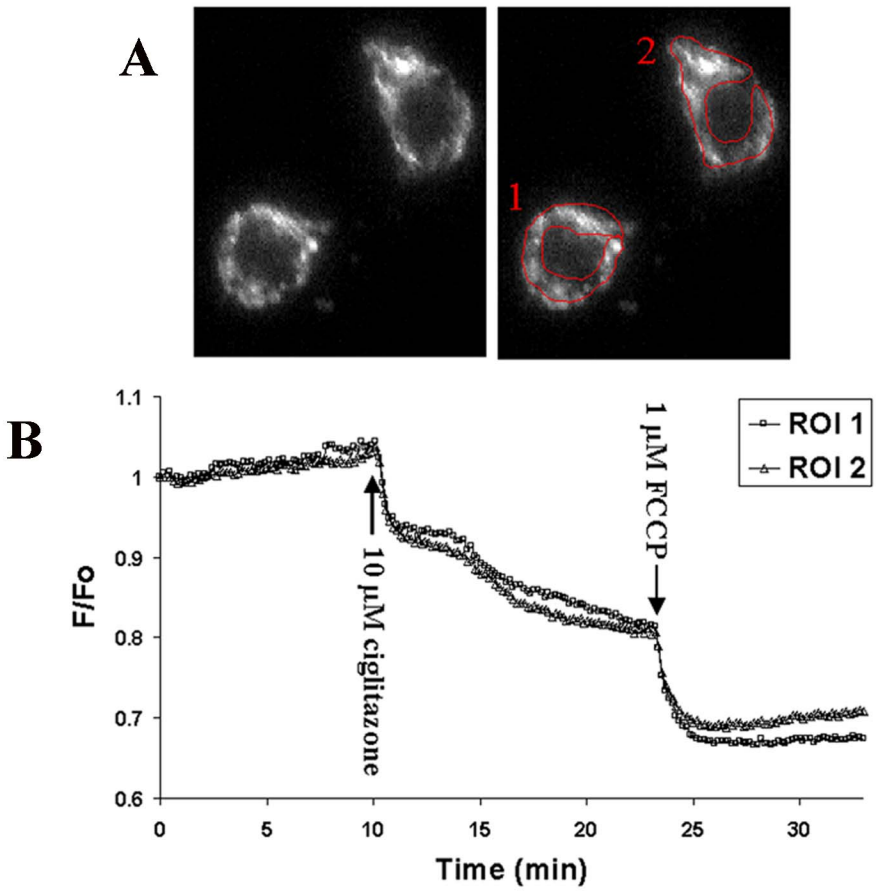

Supplemental Figure 3

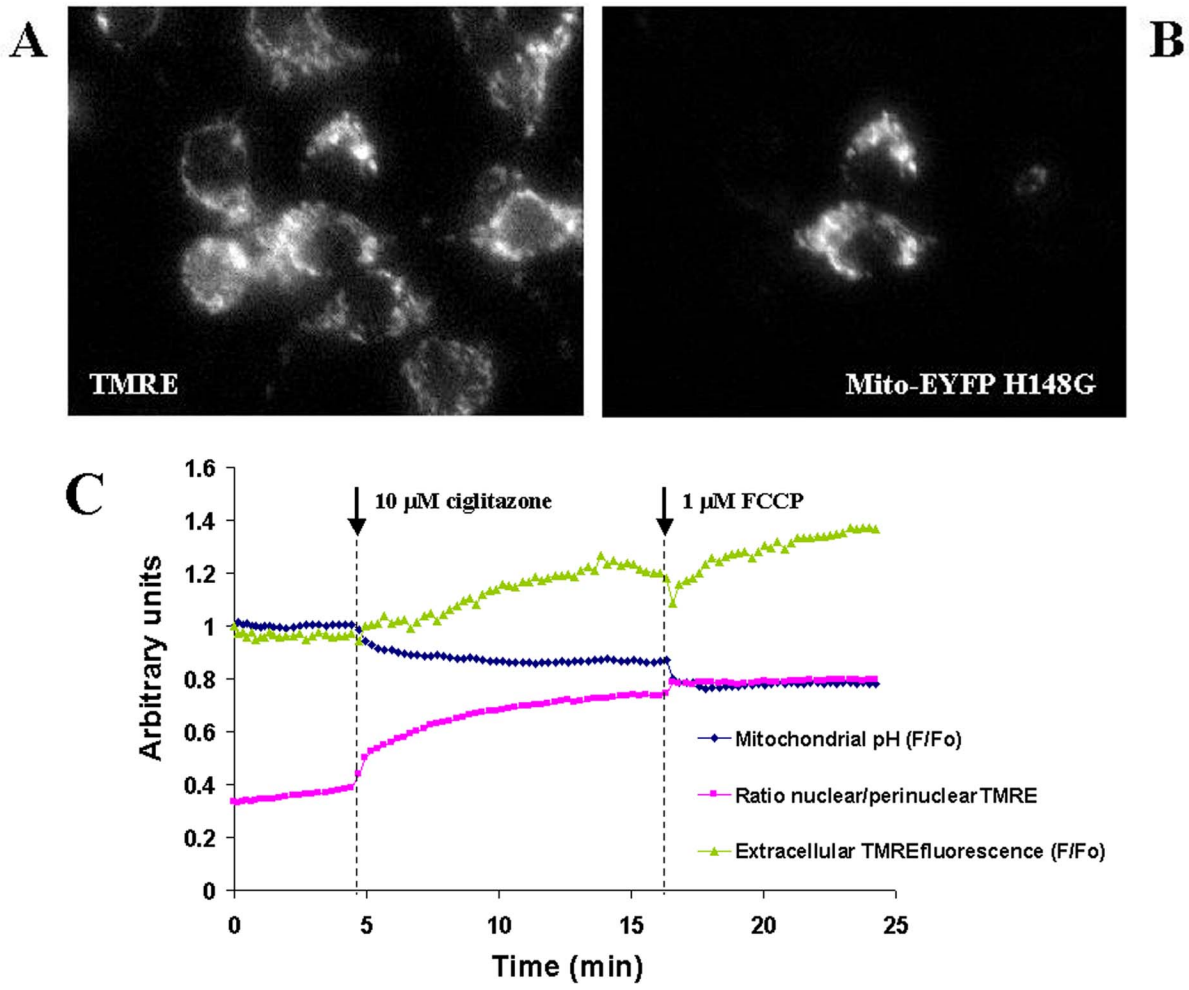

Supplemental Figure 4

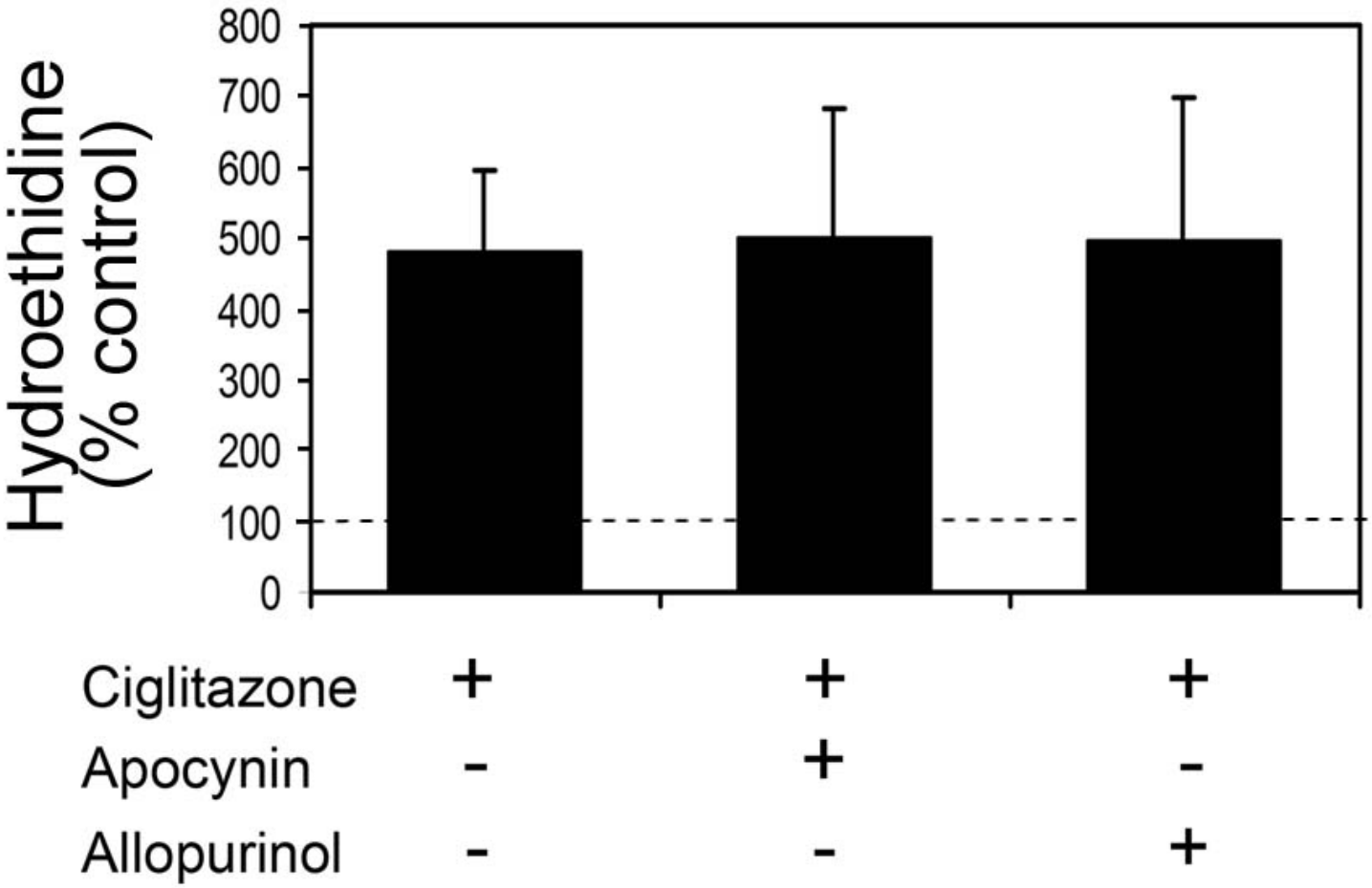

Supplemental Figure 5

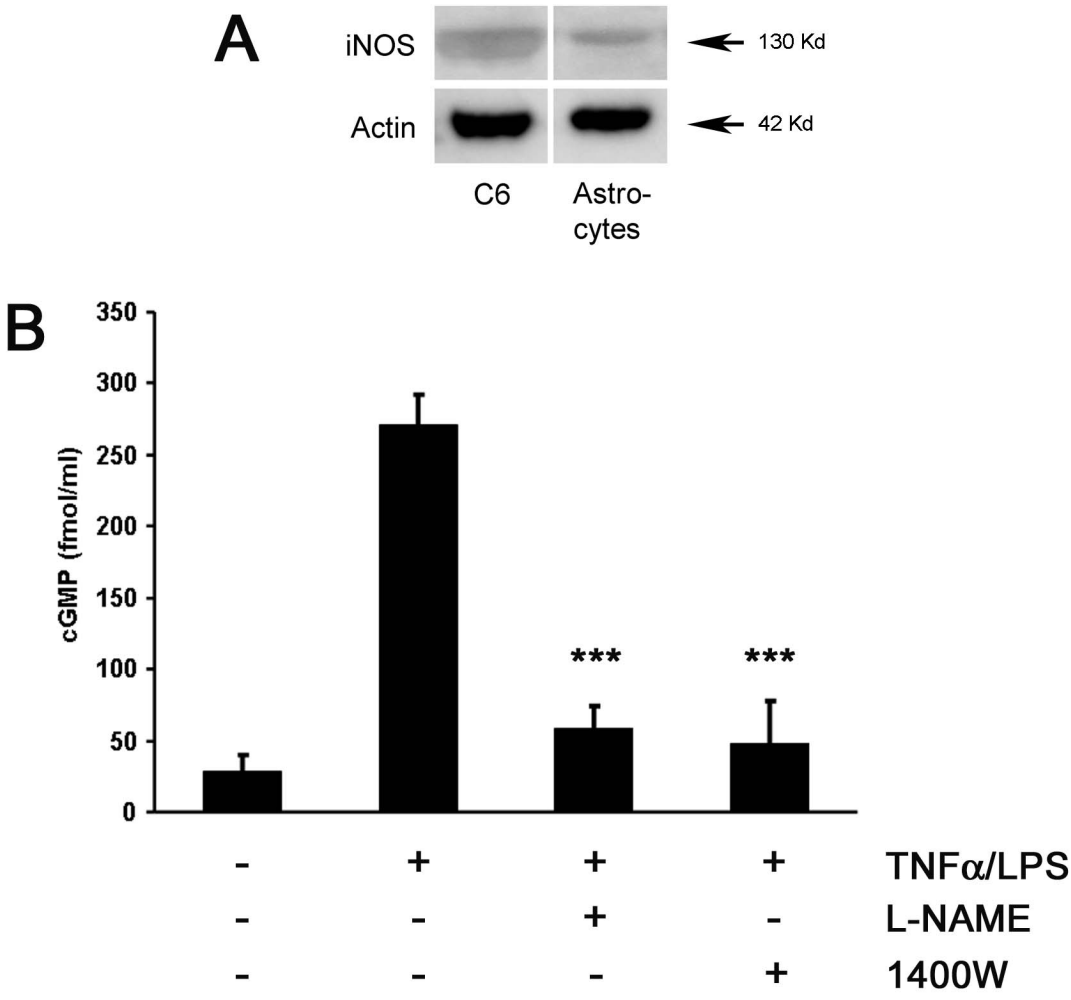

Supplemental Figure 6

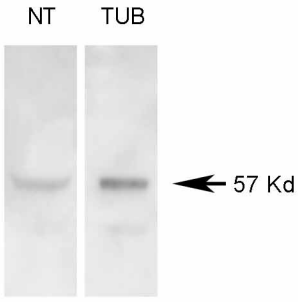

SUPPLEMENTAL DATA

Supplemental Figure 1. **Mitochondrial depolarization effect in C6 glioma cells.**

A Fluorescence microscopy images of a C6 glioma cell loaded with the potentiometric mitochondrial indicator TMRE during a time lapse experiment. Two separate regions of interest (nuclear and perinuclear) were manually drawn on a cell. TMRE stained mitochondria in the cell at rest (at time=9 min in the time course) whereas nuclear intensity remained very low. Incubation with ciglitazone (10 μM) results in a decrease of mitochondrial TMRE concentration with a rise of cytoplasmic and nuclear intensity (time=16 min), whereas the protonophore FCCP (1 μM) results in complete mitochondrial depolarization and loss of mitochondrial staining (time=36 min).

B Time-lapse experiment on the loaded cell of panel A. Fluorescence in the nuclear and perinuclear region (panel A) is expressed relative to intensity at time=0 min (F/F_0, measured fluorescence at each time point/initial fluorescence). Immediately after ciglitazone addition there was an increase in perinuclear fluorescence, owing to dequenching of mitochondrial TMRE, and a larger relative increase of TMRE fluorescence in the nuclear region. The ratio of nuclear/perinuclear TMRE intensity (expressed as R/R_0, measured ratio at each time point/initial ratio) correlates with mitochondrial depolarization.

Supplemental Figure 2. **Decrease in mitochondrial pH induced by glitazones.**

A Fluorescence microscopy images of C6 glioma cells transiently transfected with the recombinant mitochondrial pH indicator "mito-EYFP H148G". The subcellular distribution of the chimera was mitochondrial, as indicated by colocalization with the

potentiometric mitochondrial indicator TMRE. Two separate regions of interest were drawn manually on transfected cells (shown on the right panel).

B A time-lapse experiment on the transfected cells of panel A showed a stable signal corresponding to resting mitochondrial matrix pH. Incubation with ciglitazone (10 μM) resulted in a decrease of mitochondrial fluorescence with a very rapid drop (<1 min) and a slower phase, indicative of a decrease of mitochondrial pH. Fluorescence change in time is expressed as F/F_0 (measured fluorescence in each time point/initial fluorescence). The protonophore FCCP (1 μM) was subsequently added to make mitochondrial pH approximately equal to cytoplasmic pH (7-7.2 from control experiments using the pH indicator BCECF). Therefore, ciglitazone lowers cytoplasmic pH in addition to causing mitochondrial depolarization (shown in Figure 5, Supplemental Figures 1 and 3, and Supplemental Video).

Supplemental Figure 3. **Simultaneous detection of mitochondrial membrane potential and pH. Effect of ciglitazone.**

A and B Fluorescence microscopy images of C6 glioma cells transiently transfected with the recombinant mitochondrial pH indicator "mito-EYFP H148G" and loaded with the mitochondrial membrane potential indicator TMRE. All cells were labeled with TMRE (A) and two cells transfected with mito-EYFP H148G are shown (B). The green and red emission bands were separated by appropriate excitation and emission filters (see Supplemental Methods) and there was no cross-talk between the fluorophores. **C** Time-lapse experiment on the above cells. Mitochondrial pH (average of the two transfected cells) was expressed as the mito-EYFP H148G fluorescence change in time, F/F_0 (measured fluorescence in each time point/initial fluorescence). The ratio of nuclear to perinuclear TMRE fluorescence is also shown (average of 7 stained cells).

This ratio is a faithful representation of mitochondrial depolarization (Supplemental Figure 1). Finally, the extracellular TMRE fluorescence (F) divided by the value at zero time (F_0) is represented. Incubation of cells with 10 μM ciglitazone causes simultaneous decrease in mitochondrial pH and loss of mitochondrial membrane potential. At time = 16 min, FCCP (1 μM) was added, and mitochondrial pH and membrane potential decreased further.

Supplemental Figure 4. **Flow cytometry analysis of extramitochondrial ROS.**

C6 glioma cells were pre-incubated during 15 min with 0.1 mM allopurinol or 20 μM apocynin, specific inhibitors of the cytosolic enzymes xanthine-oxidase and NADPH-oxidase, respectively. Then, cells were exposed to 10 μM ciglitazone or vehicle (0.02% Me_2SO) for another 15 min period. $O_2^{\cdot -}$ production was evaluated by flow cytometry after addition of the fluorescent probe hydroethidine (5 μM) to cell cultures 5 min prior to ciglitazone treatment. Results are shown as percentage of controls (cells treated with vehicle). Data represent the mean ± S.D. from three independent experiments. None of the inhibitors used altered $O_2^{\cdot -}$ formation in response to ciglitazone.

Supplemental Figure 5. **iNOS expression and function in C6 glioma cells.**

A Western blot detection of iNOS in protein extracts from C6 cells. iNOS expression in C6 cells was compared with mouse primary astrocyte cultures as previously described (Burgos *et al.*, 2007). Membranes were incubated with anti-iNOS (1:100; BD Transduction Laboratories) or anti-β-actin (1:2000; Sigma) antibodies and probed with peroxidase-conjugated secondary antibody following manufacturer's instructions. An enhanced chemiluminescence system was used for visualization.

B Determination of cGMP levels by enzymeimmunoassay (EIA Direct cyclic GMP kit, Sigma) in control C6 cells and cells stimulated overnight with the iNOS inducers TNFα (100 ng/ml) and LPS (5 μg/ml). A 2 h preincubation with the NOS inhibitors L-NAME (500 μM) and 1400W (50 μM) was able to significantly reduce ($p<0,0001$) the cGMP formation induced by TNFα/LPS.

Supplemental Figure 6. **Nitrotyrosine and α-tubulin in C6 glioma cells.**

Western blot detection of nitrotyrosine and α-tubulin in protein extracts from C6 cells. Membranes were incubated with anti-nitrotyrosine (1:50; HyCult Bt.) or anti-α-tubulin (1:1000; Oncogene) antibodies and probed with peroxidase-conjugated secondary antibody following manufacturer's instructions. An enhanced chemiluminescence system was used for visualization.

Supplemental Video. **Mitochondrial depolarization of C6 cells by ciglitazone.**

A field with eight live C6 cells labeled with the mitochondrial membrane potential indicator TMRE is shown. In resting cells the fluorescence is mitochondrial, and flickering of this staining (transient depolarizations) are seen. Addition of FCCP (1 μM) results in release of TMRE to the cytoplasm and nucleus (the extracellular TMRE cannot be resolved by eye). When the protonophore FCCP is washed out from the bath, mitochondria regain their resting membrane potential and accumulation of TMRE is observed. Two cycles of protonophore addition and wash are shown. When ciglitazone was added to cells (10 μM), membrane potential was lost (TMRE distribution became cytoplasmic and nuclear). However, this effect was not reversed by removal of ciglitazone from the bath in the time scale of tens of minutes. The duration of the experiment shown in the clip was 60 min.

Supplemental Methods

Imaging of membrane potential with TMRE was done as indicated in the Materials and Methods section. We have previously used mitochondrially-targeted EYFP as a reporter of mitochondrial matrix pH (Llopis *et al.*, 1998). EYFP has a pKa of 7, and this value is about 1 pH unit below the prevailing pH in the mitochondrial matrix. In this study we used the mutant "EYFP H148G" (histidine 148 is replaced by the smaller glycine). The introduction of this point mutation has been shown to cause a proton channel into the fluorochrome within the YFP barrel structure (Wachter *et al.*, 1998) resulting in a pKa of 8.02 (Elsliger *et al.*, 1999), a value matching the resting pH of energized mitochondria in live cells.

The pH sensor "EYFP H148G" was targeted to the mitochondrial matrix using the N-terminal 12 aminoacids of the presequence of subunit IV of cytochrome c oxidase (Hurt *et al.*, 1985). We named this targeted chimeric protein "mito-EYFP H148G".

Imaging was done on a wide-field fluorescence microscope equipped with a monochromatic light source (Hamamatsu Photonics) able to shift excitation wavelength within tens of milliseconds. Emission filters were mounted on a Sutter Instruments filterwheel placed on a Hamamatsu Orca-ER CCD camera. For "mito-EYFP H148G" imaging, excitation was set at 480 nm, and a 505 nm dichroic and 535/26 nm bandpass emission filters were used (Omega).

SUPPLEMENTAL REFERENCES

Burgos M, Calvo S, Molina F, Vaquero C F, Samarel A, Llopis J and Tranque P (2007) PKCepsilon Induces Astrocyte Stellation by Modulating Multiple Cytoskeletal Proteins

and Interacting With Rho A Signalling Pathways: Implications for Neuroinflammation. *Eur J Neurosci* **25**:1069-1078.

Elsliger MA, Wachter R M, Hanson G T, Kallio K and Remington S J (1999) Structural and Spectral Response of Green Fluorescent Protein Variants to Changes in PH. *Biochemistry* **38**:5296-5301.

Hurt EC, Pesold-Hurt B, Suda K, Oppliger W and Schatz G (1985) The First Twelve Amino Acids (Less Than Half of the Pre-Sequence) of an Imported Mitochondrial Protein Can Direct Mouse Cytosolic Dihydrofolate Reductase into the Yeast Mitochondrial Matrix. *EMBO J* **4**:2061-2068.

Llopis J, McCaffery J M, Miyawaki A, Farquhar M G and Tsien R Y (1998) Measurement of Cytosolic, Mitochondrial, and Golgi PH in Single Living Cells With Green Fluorescent Proteins. *Proc Natl Acad Sci U S A* **95**:6803-6808.

Wachter RM, Elsliger M A, Kallio K, Hanson G T and Remington S J (1998) Structural Basis of Spectral Shifts in the Yellow-Emission Variants of Green Fluorescent Protein. *Structure* **6**:1267-1277.